

# Assessment of meteorological settings on air quality modeling system - a proposal for UN-SDG and regulatory studies in non-homogeneous regions in Brazil

**Mauricio Soares da Silva** (✉ [soares@lamma.ufrj.br](mailto:soares@lamma.ufrj.br))

Federal University of Rio de Janeiro: Universidade Federal do Rio de Janeiro <https://orcid.org/0000-0002-1163-993X>

**Luiz Cláudio Gomes Pimentel**

Federal University of Rio de Janeiro: Universidade Federal do Rio de Janeiro

**Fernando Pereira Duda**

Federal University of Rio de Janeiro: Universidade Federal do Rio de Janeiro

**Leonardo Aragão**

Alma Mater Studiorum Universita di Bologna: Universita di Bologna

**Corbiniano Silva**

Federal University of Rio de Janeiro: Universidade Federal do Rio de Janeiro

**Ian Cunha D'Amato Viana Dragaud**

Federal University of Rio de Janeiro: Universidade Federal do Rio de Janeiro

**Pedro Caffaro Vicentini**

Currently without affiliation



---

## Research Article

**Keywords:** Air Quality Modeling, Regulatory Purpose, SGDs, WRF, CALMET, CALPUFF, Metropolitan Regions

**Posted Date:** January 13th, 2022

**DOI:** <https://doi.org/10.21203/rs.3.rs-1108966/v1>

**License:**   This work is licensed under a Creative Commons Attribution 4.0 International License. [Read Full License](#)

---

# Abstract

Air quality models are essential tools to meet the United Nations Sustainable Development Goals (UN-SDG) because they are effective in guiding public policies for the management of air pollutant emissions and their impacts on the environment and human health. Despite its importance, Brazil still lacks a guide for choosing and setting air quality models for regulatory purposes. Based on this, the current research aims to assess the combined WRF/CALMET/CALPUFF models for representing SO<sub>2</sub> dispersion over non-homogeneous regions as a regulatory model for policies in Brazilian Metropolitan Regions to satisfy the UN-SDG. The combined system was applied to the Rio de Janeiro Metropolitan Region (RJMR), which is known for its physiographic complexity. In the first step, the WRF model was evaluated against surface-observed data. The local circulation was underestimated, while the prevailing observational winds were well-represented. In the second step, it was verified that all CALMET three meteorological configurations performed better for the most frequent wind speed classes, so that the largest SO<sub>2</sub> concentrations errors occurred during light winds. Among the meteorological settings in WRF/CALMET/CALPUFF, the joined use of observed and modeled meteorological data yielded the best results for the dispersion of pollutants. This result emphasizes the relevance of meteorological data composition in complex regions with unsatisfactory monitoring given the inherent limitations of prognostic models and the excessive extrapolation of observed data that can generate distortions of reality. This research concludes with the proposal of the WRF/CALMET/CALPUFF air quality regulatory system as a supporting tool for policies in the Brazilian Metropolitan Regions in the framework of the UN-SDG, particularly in non-homogeneous regions where steady-state Gaussian models are not applicable.

## 1. Introduction

Cities are important agents of change to build actions that identify virtues and vulnerabilities, as evidenced in the 17 Sustainable Development Goals (SDG) of the 2030 Agenda of the United Nations (UN) (UN, 2015), contributing to the environmental and life quality of the population worldwide and tackling key challenges established in the global pact signed by 193 UN member states, including Brazil (UN, 2015; 2018).

According to WHO (2016), air pollution represents the most significant environmental risk to health and affects all regions, scenarios, socioeconomic and age groups. Every year, about 4.2 million deaths worldwide are attributed to ambient air pollution, and 91% of the world's population lives in places exceeding WHO air quality guidelines. Consequently, approaches seeking out an improving air quality are directly connected with access to clean energy services, climate mitigation goals, waste management, and other aspects of socioeconomic development (UN 2015, 2018; Rafaj et al. 2018).

Modeling tools are important strategies for environmental analysis, land occupation effects on urban regions and megacities, to guide public policies in the air pollutant emissions control and their impacts on the air quality and population health in the context of the UN SDGs (*e.g.* US EPA 2005; Wang 2012; Requia et al. 2016; Ajtai et al. 2019; Chen et al. 2019; Higgins et al. 2019). The use of Air Quality (AQ) models is a complementary strategy to environmental monitoring and provides information to estimate the adverse impacts caused by gaseous emissions from industrial, vehicular, and other sources over health and ecosystems. The AQ models are the only method diagnostic and/or prognostic that quantifies the deterministic relationship between emissions sources and concentrations/depositions at the receptor, making it possible to define and evaluate the effectiveness of mitigation strategies (Daly and Zannetti 2007). Such computational platforms with georeferencing techniques

enable efficient implementation of environment and health management program, based on air pollution episodes, spatial detailing of the pollutants concentration, and delimitation of the impact area, assist in the optimized design of the environmental monitoring network (EEA 2011).

Despite all the potentialities of the AQ models, these tools have uncertainties sources known associated with meteorological fields, physical-chemical parameterizations, and emission inventory (Ap Simon et al. 2002; Holnicki and Nahorski 2015; Haupt et al. 2019a,b), which should be minimized through sensitivity and performance studies.

Regarding the meteorological fields, the use of diagnostic and prognostic computational modeling has constituted an alternative to complement or replace observational weather information to the AQ models (Lalas and Ratto 1996; Chandrasekar et al. 2003; Jackson et al. 2006; Abdul-Wahab et al. 2011a; De Visscher 2013; Lee et al. 2014; Wu et al. 2017; Rzeszutek 2019; Haupt et al. 2019a).

It is worth highlighting those diagnostic models such as, California Meteorological Model (CALMET), Quick Urban and Industrial Complex (QUIC) (Pardjajak and Brown 2003), Stationary Wind Flow and Turbulence (SWIFT) (Geai 1975), and MCSCIPUF (Sykes et al. 1984), do not represent a full solution to the atmospheric governing equations and cannot forecast atmospheric conditions since they are not elaborated through the time integration of the conservation equations (Lalas and Ratto 1996). Prognostic atmospheric models or Numerical Weather Prediction (NWP) models as the Fifth-generation Pennsylvania State University - NCAR Mesoscale Model - MM5 (Dudhia 1993), Advanced Regional Prediction System (ARPS) (Chow 2006), and the Weather Research and Forecasting (WRF) model (Skamarock et al. 2019) are based on the solution of mass, momentum, and heat conservation equations. Although significant improvements have been made in the NWP models, some deficiencies remain, such as high computational costs, the difficulty in representing microscale effects, ample use of physical parameterizations to represent the atmospheric process and difficulties in representing non-homogeneous boundary layer (e.g. Chow 2006; Paiva et al. 2014; Dragaud et al. 2019; Rzeszutek 2019).

Klausmann et al. (2003) combined the ETA/CALMET/CALPUFF models to represent the dispersion and deposition of radioactive pollutants in situations with little meteorological information. Pfender et al. (2006) operated the MM5/CALMET/CALPUFF models to simulate the transport and deposition of phytopathogenic fungi spores. Aiming at estimating the impacts of air quality on the city of Chongqing, China. Yang et al. (2008) utilized the MM5/CALMET/CALPUFF in the transport of SO<sub>2</sub> to supplant the lack of measured meteorological data. Yim et al. (2010) using the MM5/CALMET/CALPUFF models were capable of reproducing regional monsoon patterns in Hong Kong making it possible to observe the variability of SO<sub>2</sub> concentrations during summer and winter seasons. Abdul-Wahab et al. (2011b) investigated the SO<sub>2</sub> dispersion in the coastal region of Oman with WRF/CALMET/CALPUFF. Cui et al. (2011) evaluated the MM5/CALMET/CALPUFF models for a tracer experiment with synoptic conditions favorable for light winds in a complex terrain setting. Besides the detailed studies, other more recent investigations available in the scientific literature seek to demonstrate the skill of the atmospheric combined models to represent the wind field in high resolution into the pollutant dispersion model (Hernández-Garces et al. 2015; Hao Wu and Qi Yu 2018; Rzeszutek 2019).

The AQ models are still not explored by the Brazilian legislation as an air quality control strategy to urban, regional, or all over the country. Despite the diversity of AQ models available in the international literature in recent years (Holmes and Morawska 2006; Leelőssy et al. 2014; Aggarwal et al. 2014; Oliveri Conti 2017), its use

foreseen by Brazilian environmental agencies within the scope of the states or country has been restricted to the isolated assessment of atmospheric emissions impact from industrial enterprises of aiming at the granting of environmental licensing. It is noteworthy that, even for regulatory use, the National Air Quality Control Program (PRONAR) and its resolutions from 1989, 1990 and 2018, have not established a standard for choosing the AQ models, as well as its settings for the various Brazilian metropolitan regions. For this reason, steady-state and homogeneous models (*e.g.* ISC (USEPA 1995) and AERMOD (USEPA 2004)) are used even in non-applicable conditions, such as under complex terrain. On the other hand, models such as CALPUFF (Scire et al. 2000b), SCIPUFF (Sykes et al. 1996), and GRAL (Oettl 2013) represent the influence of other atmospheric phenomena that vary in space-time (*e.g.* fumigation, breeze, mountain circulations), besides not demand high computational costs and many inputs such as the WRF-Chem (Grell et al. 2005) and CMAQ (Byun and Schere 2006) models that are still not feasible for regulatory purposes. Appropriate AQ models for the licensing of the ports, oil exploration activities, highways, and airports still must be established in the state and/or federal legislation.

The current scenario is worrying due to the disordered expansion of urban-industrial areas in the country and the consequent increase in the concentration levels of atmospheric pollutants such as particulate matter and ozone (Silva and Pimentel 2017; Da Silveira et al. 2021). The RJMR is the second largest among the 74 metropolitan areas in Brazil (IBGE 2020) and presents the second-highest concentration of industries and vehicles in the country (INEA 2015). These aspects in conjunction with the heterogeneity of land use and land cover, and anthropogenic source location, wind regime spatial and temporal variability, and complex topography play an important role in the atmospheric pollutant dispersion modeling in the non-homogeneous Rio de Janeiro Metropolitan Region (RJMR) (Pimentel et al. 2014a, b; Paiva et al. 2014; Silveira et al. 2021). Also valuable is the use of AQ models to design and support the local observation network and depict violations of air quality standards, as well as to establish and guide public policies for urban - industrial planning and RMRJ environmental protection areas (Silveira et al. 2021).

The lack of observed meteorological information in various regions of Brazil has led certain environmental agencies to recommend the use of results from prognostic atmospheric models as a manner of superseding this absence for use in regulatory models of air quality. Among the many available models, the WRF (Skamarock et al. 2019) has been frequently recommended for this purpose. However, as discussed in Rzeszutek (2019), meteorological and air quality modeling in complex terrains is one of the main challenges nowadays. This argument is valid for the RJMR, as verified by previous studies on the simulation of pollutants dispersion and atmospheric flow over the surface in this region (Pimentel et al. 2014b; Paiva et al., 2014). Care must be taken to obtain predictions with a universal configuration for the NWP models, as proposed by State Environmental Institute (INEA), and the selection of input data of adequate quality for different regions.

This study aims to evaluate meteorological settings of the combined WRF/CALMET/CALPUFF models to represent the dispersion of SO<sub>2</sub> in hourly and 24-hour time scales over non-homogeneous regions as a proposition to a regulatory model for land use policies in Brazilian Metropolitan Regions in the context of UN Sustainable Development Goals - 2030 Agenda.

## 2. Study Area

The RJMR comprises 22 cities, with a territory of 7530.386 km<sup>2</sup>, a population about 13 million, and a density of 1743.81 inhab·km<sup>-2</sup> and is currently the second largest among the 74 metropolitan areas in Brazil (IBGE 2020). It

is a highly industrialized region, whose current process has been leveraged by the metal-steel and logistical-oil sectors, integrated with other industries and their associated activities, and increased by logistical investments (articulated by highways, railways, and ports) and industrial, productive partnerships, financial and tax with the installed companies. The RJMR is characterized as a pole of attraction of investments and expansion of already consolidated sectors and the newer ones, where the Rio de Janeiro Petrochemical Complex (COMPERJ) and the enterprises located in the Sepetiba Bay (Porto de Itaguaí, Ternium, Gerdau, Usiminas, Petrobrás, LLX, among others) stand out.

According to the criteria established by the State Environmental Institute (INEA 2010, 2015), the leading industrial activities in the Rio de Janeiro state are of high or medium potential for pollution, with RJMR being the one with the highest levels of air quality degradation. It occurs mainly due to the high concentration of emission sources since it is the second-largest concentration of vehicles, industries, and polluting sources in the country, whose consequences generate severe problems of air pollution. In the report INEA (2010), it was highlighted that this region showed the greatest compromise in air quality in the Rio de Janeiro State, being 77% of all inventoried emitted pollutants from vehicular sources, and 23% coming mostly from industrial sectors like petrochemical, naval, chemical, food, and energy transformation.

Its geo-bio-physiographic characteristics enhance problems associated with air quality and are challenging elements for atmospheric modeling studies: rugged topography; proximity to the sea (Atlantic Ocean) and the presence of water bodies (Guanabara and Sepetiba bays, beyond lakes) that, together, produce a complex and heterogeneous airflow in terms of the distribution and dispersion of pollutants; the tropical climate, which favors photochemical processes, generating others pollutants; as well as the critical and intense process of land use, which highlights urban and industrial areas, and the largest urban forest on the planet (Tijuca Forest), among other uses (Figure 1 and Figure 2).

The RJMR is under the influence of the South Atlantic Subtropical Anticyclone (SASA) throughout the year, which induces clear and slightly cloudy skies (Dereczynski and Menezes 2015). The influence of SASA is interrupted by transient weather systems, such as extratropical cyclones, frontal systems, mesoscale convective systems, upper tropospheric subtropical cyclonic vortices, and South Atlantic Convergence Zone (SACZ), which promote increased cloudiness and rainfall (Dereczynski and Menezes 2015). The near-surface flow is driven by land-sea and bay breeze circulations and presents a wind pattern perpendicular to the coastline (Pimentel et al. 2014a; Aragão et al. 2017; Dragaud et al. 2019). Under the influence of an atmospheric frontal system, winds come from the southern quadrant (Stech and Lorenzetti 1992; Dourado and Oliveira 2000) and inhibit the local circulations.

Pollution and air quality are identified in connection with the SDGs (UN 2018) and have been incorporated into the RMRJ municipalities. The SDGs directly related to air pollution (WHO 2016) include: health (SDG 3, target 3.9), cities (SDG 11, target 11.6), and energy (SDG 7, target 7.A). Air quality is implicit in other development goals: food production and safety (SDG 2, target 2.4); economic growth and employment (SDG 8, target 8.4); reduced inequality (SDG 10); urgent actions to mitigate climate change (SDG 13, target 13.2); conservation and sustainable use of oceans, seas and marine resources (SDG 14, target 14.1); sustainably manage of forests, combat desertification, halt and reverse land degradation, face the biodiversity loss (SDG 15, targets 15.1, 15.4, and 15.5).

The methodology is based on the implementation of the Sustainable Cities Development Index - Brazil (IDSC-BR) (<https://idsc-br.sdgindex.org/methodology>), produced by the Sustainable Development Solutions Network (SDSN) (Lafortune et al. 2018). The scores highlight the largest challenges and evaluate the performance of services and public policies implemented by municipal management. The evaluation of the evolution of the municipalities in an indicator is measured in four intervals, where the green category (> 60 - 100) indicates that the municipality has reached the SDG, yellow (50 - 60) indicates that there are challenges, orange (40 - 50) indicates significant challenges, and red (< 40) indicates major challenges. Based on the adopted methodology, only 2 of the 21 RMRJ cities evaluated reached the SDGs associated with pollution and air quality, with the others in different situations of vulnerability, where 12 present challenges, 6 - significant challenges, and 1 - major challenges (Fig. 2).

## 3. Materials And Methods

### 3.1. Period

The study period was from January 1st to May 31st, 2011, defined by simultaneous availability of the required datasets (meteorological, air quality, and emissions), which comprises the main meteorological systems acting over the RJMR: the SASA, atmospheric frontal systems, SACZ, mesoscale convective systems, and breezes.

### 3.2. Observed data

Data recorded in three types of monitoring stations were used: meteorological, pluviometric, and air quality (Figure 2). Meteorological data was recorded in five World Meteorological Organization standard stations located in the airports of RJMR. From the five stations – Galeão Airport (SBGL), Campos dos Afonsos Airport (SBAF), Santos Dumont Airport (SBRJ), Jacarepaguá Airport (SBJR), and Santa Cruz Airport (SBSC) – only the SBGL station registers both surface and upper-air observations. At surface level, the records are hourly, and at the upper air two soundings are launched daily at 9 a.m. and 9 p.m. local time. Three surface stations (SBGL, SBAF, and SBSC) operate on a full-time basis, that is, 24 hours a day, while the SBRJ and SBJR stations operate from 6 a.m. to 11 p.m. and 6 a.m. to 10 p.m. local time, respectively. The wind data used in this study presents measurements above  $0.5 \text{ m}\cdot\text{s}^{-1}$  ( $\approx 1$  knot). Wind speed values below this threshold are considered calm winds. To elaborate on the diagrams, the wind classes defined in the Beaufort scale were considered (WMO 2018).

In addition to traditional meteorological stations, 41 pluviometric stations with hourly accumulated rainfall data are considered to represent the wet removal mechanism. 32 stations come from the Municipality of Rio de Janeiro network and 9 from the State of Rio de Janeiro network (Figure 2). The AQ monitoring stations present in the RJMR are carried out by INEA (State Institute of the Environment), SMAC (Secretariat of Environment of the Municipality of Rio de Janeiro), in addition to several private companies. This study considers hourly averages of  $\text{SO}_2$  concentrations from five AQ monitoring stations: Copacabana, São Cristóvão, Tijuca, Jardim Primavera, and São Bento (Figure 2). The first three are managed by SMAC and the last two by private companies. Although there are more AQ stations for the study period, only the stations with 75% or more recorded data were considered.

### 3.3. WRF Model and uncertainty thresholds for the evaluation of wind speed.

Due to the advances in solution techniques, improvements to the representation of physical processes, and an increase in computational power, prognostic models currently represent state-of-the-art approaches to simulating atmospheric phenomena in various time-space scales (Pielke 2002; Goger et al. 2016; Yano et al. 2018; Haupt et al., 2019a, b, c).

The WRF is an NWP model developed for operational purposes and atmospheric research (Skamarock et al. 2019). Initial and boundary conditions used in the simulations were produced with the Global Forecasting System (GFS) model, which generates analysis with a horizontal spatial resolution of  $0.5^\circ$  ( $\sim 55$  km at RJMR latitudes) and a temporal resolution of 6 hours. Four nested domains centered on the Rio de Janeiro state were adjusted with one-way interaction (Figure 3). The largest domain, D1, possesses 24 km of horizontal grid resolution with  $130 \times 100$  grid cells, the second domain (D2) has an 8 km grid resolution with  $148 \times 106$  grid cells, the third (D3) has a 2.666 km grid resolution with  $172 \times 112$  grid cells, and the last one, D4, has a 0.888 km grid resolution with  $181 \times 112$  grid cells, covering the whole RJMR. All domains have 45 vertical levels, from the ground level up to 50 hPa. The physics parameterization schemes used and generally recommended by environmental agencies in Brazil are Rapid Radiative Transfer Model for General Circulation Models (RRTMG) (Iacono et al. 2008), Revised MM5 (Jimenez et al. 2012a), Noah – MP Land Surface Model (Niu et al. 2011), Yonsei University (YSU) (Hong et al. 2006), WRF single-moment three-class (WSM3) (Hong et al. 2004) and Kain–Fritsch Scheme (Kain 2004). The horizontal diffusion was computed in physical space since it is more realistic and suggested for regions with complex terrain (Chen 2020).

Several studies have been developed to evaluate the accuracy of atmospheric models through the comparison with observational data using statistical indexes, as bias and RMSE (Root-Mean-Square Error) (*e.g.* Hanna and Yang 2001; Chow 2006; Zhang et al. 2011; Paiva et al. 2014; Yver 2013). However, there are different uncertainty levels not only by the setups applied on models (*e.g.* schemes, grids, initial and boundary conditions) but also due to the geographical complexity that influences the wind regimes. In the Table 1 and Table 2 are summarized the uncertainty thresholds for the evaluation of wind speed.

Table 1. Summarized statistical indexes for wind speed and wind direction.

Studies	Index	Wind Speed (ms <sup>-1</sup> )		Wind Direction (°)		Ideal
		Best	Worst	Best	Worst	
Hanna & Yang (2001)	RMSE	1.6	2.5	51	76	0
	bias	-0.1	1.5	-2	-14	0
Zhang et al. (2011)	RMSE	2.6	3.7	172.6	193.4	0
	bias	1.4	2.5	-20.9	-80.9	0
Paiva et al. (2014)	RMSE	1.12	4.26	59.73	105.11	0
	bias	0.03	3.18	2.56	-36.47	0
Chow et al. (2006)	RMSE	0.53	1.56	53.14	93.21	0
	bias	0.04	-1.01	-1.50	-35.79	0
Yver et al. (2013)	RMSE	1.00	3.00	40.00	140.00	0
	bias	-	-	-	-	0

Table 2. Uncertainty grades for wind speed, according to Clifford (2011).

Grade	RMSE (m.s <sup>-1</sup> )	MAE (m.s <sup>-1</sup> )
Poor	> 3.0	> 3.0
Acceptable	< 3.0	< 3.0
Good	< 2.5	< 2.5
Excellent	< 2.0	< 2.0

### 3.4. CALPUFF Modeling System

The California Puff Model (CALPUFF) modeling system consists of two main processing modules and a post-processing one: the meteorological module CALMET, the dispersion module CALPUFF and the CALPOST. The latter is responsible for the post-processing of the results generated by the CALMET and CALPUFF modules (Scire et al. 2000a, b). CALMET is a diagnostic meteorological model that produces a 3D gridded field of wind and temperature, estimates micrometeorological parameters (for input in the CALPUFF dispersion model), and assures mass conservation, being called a mass-consistent model (Scire et al. 2000a). The relative simplicity and operability of diagnostic models, combined with the skill to run much faster than prognostic models, make them attractive for many practical purposes. It should also be considered that these models do not require much input data available to operate efficiently into the generation of a 3D gridded meteorological field, which satisfies some physical constraints as kinematic terrain effects, slope flows, and blocking effects (Lalas and Ratto 1996; Scire et al. 2000a; Haupt et al. 2019a, b, c).

The domain utilized in CALMET was adjusted to cover the largest part of the RJMR: 160 x 140 horizontal grid cells with 0.5 km of resolution (Figure 1 and Figure 2) and 12 vertical layers from the ground level up to the free atmosphere (4000 meters). Topography data from the Shuttle Radar Topographic Mission project (Farr et al. 2007) were used with 90-meter of spatial resolution, as well as soil use and occupation data from the Glob Cover



project (Defourny et al. 2006) with a 300 m resolution. The required parameters TERRAD, R1, RMAX1, R2, and RMAX2 were set with the values 10 km, 1 km, 2 km, 10 km, and 20 km, respectively.

To define the best meteorological setting in the WRF/CALMET/CALPUFF, three numerical experiments were developed:

- CONFIG 1: Meteorological data measured at five surface meteorological stations, one upper air meteorological station, and 41 precipitation stations.
- CONFIG 2: Meteorological data from WRF model and 41 precipitation stations.
- CONFIG 3: Combination of the data used in CONFIG 1 and CONFIG 2.

Since the evaluation period is long and includes rainy conditions, all simulations considered the wet removal process using the standard CALPUFF coefficients (Scire et al. 2000b), and the rainfall data measured in 41 stations. To avoid errors associated with the WRF precipitation field and to allow a more focused assessment on the wind, only measured data were employed, including CONFIG 2.

Before being used in the CALMET model, the WRF information was pre-processed by the CALWRF, a code also developed and distributed by the developers of the CALPUFF modeling system.

The CALPUFF model (Scire et al. 2000b) is a multi-layer, multi-species, non-steady-state Lagrangian modeling system of the atmospheric dispersion of puffs with Gaussian distribution. Its main characteristics are the capacity to simulate the effects of time and space varying meteorological conditions, calm wind conditions, first-order chemical transformations, and removal processes during transportation. The method based on the Similarity Theory was used to calculate the dispersion coefficients, and the method considered for the representation of the plume was the *Slug* (non-circular puff elongated in the direction of the wind when near its source).

### **3.5. Sulfur Dioxide Total Emissions at RJMR**

The primary pollutant sulfur dioxide (SO<sub>2</sub>) was employed in the present study, where the inventory of fixed and mobile emissions used in the data entry process of WRF/CALMET/CALPUFF is the same one utilized by Vicentini (2011) and Vicentini et al. (2011). In the latter study, all sulfur dioxide fixed and mobile sources of the RJMR were considered according to the INEA pollutant emission inventory prepared in 2009, based on the year 2008 (Vicentini 2011; Vicentini et al. 2011). It is noteworthy that fixed sources are responsible for about 88% of SO<sub>2</sub> emissions in RMRJ (Vicentini 2011; INEA 2010).

The inventory of fixed sources for the RJMR updated in 2009 considered the details of the inventory of the ninety largest companies out of the 425 considered in the inventory of 2003 (Pires 2005), maintaining the other companies' emission factors. All of these were treated as point sources, totaling 1917 anthropogenic fixed sources.

The inventory of mobile sources was also updated and expanded in 2009, adding to the 260 sources initially registered (2003) another 290 relating to secondary roads. The flow on the inventoried roads was measured using counts of light and heavy vehicle traffic at certain times of the day based on the manual of the National Department of Transport Infrastructure (DNIT 2006) and data from the Department of Transport of the Rio de

Janeiro (DETRAN-RJ). The RJMR's hourly variation of vehicular traffic was represented considering 24 emission factors. These factors make no distinction between weekend days 'and business days' traffic.

This inventory was formatted to be assimilated into CALPUFF, resulting in 499 area sources representing the main traffic routes in the RJMR, and 492 point sources representing the main industrial sources cataloged in the region. Figure 4 shows the areas with the highest emissions from fixed sources divided by 5 x 5 km areas. However, it should be noted that these emissions were configured in the CAQMS as point sources. Although the emission factors for fixed sources may vary over time, this variation was not considered since it would require information that is not available. Furthermore, the main emission activities in the region operate continuously under constant load most of the time.

### **3.6. Evaluation of Combined WRF/CALMET/CALPUFF system**

Even with the advances, NWP models still do not satisfactorily resolve local flow forced by terrain characteristics such as the topography and land use, for example. Otherwise, diagnostic models can better represent microscale phenomena but do not provide predicted meteorological fields (Lalas and Ratto, 1996). As an attempt to attain the best performance of the AQ models, both approaches can be combined, exploring the complementarity of their skills, comprising the so-called Combined Air Quality Modeling System (CAQMS).

The evaluation of the CAQMS skill to simulate the wind field and SO<sub>2</sub> hourly and 24-hour averages concentration was done through two steps. The first one focused on the evaluation of the WRF skill to simulate the wind field over the non-homogeneous RJMR. In this step, WRF hourly data of wind speed and direction were extracted using the nearest neighbor technique for the five meteorological surface stations. Thus, simulated and observed data were evaluated via frequency distribution diagrams (wind roses) and statistical indexes. The literature on the performance of prognostic meteorological models proposes a wide variety of statistical methods for model evaluation. However, the indexes Root Mean Square Error (RMSE), Mean Absolute Error (MAE), and bias are commonly utilized in these evaluations to quantify the uncertainty of the models (Hanna and Yang 2001; Chow et al. 2006; Zhang et al. 2011; Paiva et al. 2014).

The second step evaluated the different meteorological settings strategies used on the CAQMS - CONFIG1, CONFIG2, and CONFIG3 - modified the SO<sub>2</sub> hourly and 24-hour average concentrations results. This analysis compares the simulated results and the AQ monitoring stations data using a set of statistics indexes widely employed on AQM assessments: bias, Normalized Mean Square Error (NMSE), Pearson Correlation Coefficient (R), Factor Of EXcedance (FOEX), Factor of 2 (FA2), and Factor of 5 (FA5). In particular, FOEX was used to bring information about the percentage of samples overestimated/underestimated by the model without considering the magnitude of this error. The FOEX ranges between +50% and -50% and the ideal value is 0%. While a FOEX equal to +50% means that all values are overpredicted, a FOEX equal to -50% means that all values are under-predicted. Since FA2 (FA5) represents the percentage of estimates between  $1/2$  ( $1/5$ )  $\leq$  Observed/Predicted  $\leq$  2 (5) (Mosca et al. 1998).

## **4. Results And Discussion**

### **4.1. Analysis of the WRF skill to simulate the wind field**

Figures 5-9 present the frequency distribution diagrams of the wind data extracted from the simulations with the WRF model and from the data measured in the respective surface meteorological stations.

At the Galeão station, the most frequently observed wind directions were East and Southeast (Figure 5), associated with the afternoon-occurring sea breeze and bay breeze, as highlighted in Pimentel et al. (2014a). The results obtained with the WRF indicate that the model represents the prevailing wind directions at a frequency like those observed at the Galeão station (Figure 5). This result is above expectations since the representation of the wind at the SBGL station is difficult because it is located on an island within Guanabara Bay (Figure 2), where the breeze acts in different directions in a short distance, following the irregular shoreline. Regarding the wind speed, the observed winds in all directions are more intense than the simulated, (Figure 5), in general, and this difference in intensity occurs in the order of one class, that is, approximately  $1.5 \text{ m.s}^{-1}$ , which is excellent considering the scales of uncertainties proposed by Clifford (2011) (Table 2). For calm winds, the model results represent a percentage (4.86%) close to that observed (6.96%).

At the Campo dos Afonsos station (Figure 6), there are mainly observed winds from the south, related to the sea breeze which enters over the continent and is channeled by the Tijuca and Pedra Branca massifs (Pimentel et al. 2014a). The incidence of light winds with around 14% of calm winds, which usually occur during the night, early morning, and morning periods (Pimentel et al. 2014a), can also be highlighted. The results obtained with the WRF demonstrate that the model was able to reproduce wind patterns like those registered at the SBAF station (Figure 6). It is possible to recognize the ability of the model in the reproduction of the variability of wind directions, indicating its sensibility in simulating the coupling of processes in several scales: micro, mesoscale, and synoptic, which result in the wind regime in this region. It is also noteworthy that the frequency of the prevailing winds, the winds from the south, are like those recorded at the station, around 20% (Figure 6). Likewise, the simulated frequency of the calm winds indicates the optimal accuracy of the model (Figure 6). Regarding the wind speed, subjectively, it can be said that the results are consistent with the observed data indicating excellent performance according to criteria given by Clifford (2011) and thus being better than the results modeled for the SBGL station.

According to Pimentel et al. (2014a) the Santos Dumont (SBRJ) station (Figure 7), situated at the entrance of the Guanabara bay, suffers a strong influence from the land and sea breezes regime, where the directions South (sea breeze) and North (land breeze) are predominant. However, since the observational data available for this study were registered only during the period of 6 a.m. to 11 p.m. local time, it was not possible to observe the action of the land breeze (North winds) in the same proportion as the sea breeze (Figure 7). In the simulated results, the predominant winds are southerly winds as well as the observed data, but 10% less often (Figure 7). This difference between the observed and modeled frequency is balanced by the southeast winds, which are modeled at a frequency of approximately 10% higher than those observed (Figure 7). From this, it is assumed that the model can represent the sea breeze phenomenon at the same frequency as that observed. It is noteworthy that the second most frequent phenomenon at the station was also modeled by WRF, that is, the land breeze associated with the north winds (Figure 7). Still, about this site, the intensity of the most frequent winds varied between  $3.6 \text{ m.s}^{-1}$  and  $5.7 \text{ m.s}^{-1}$  for both observed and modeled results (Figure 7). As well as the results obtained for SBGL and SBAF, the performance of WRF to model periods of calm winds on the SBRJ site is excellent, with only about a 1% difference between those registered at the station.

For Jacarepaguá station, which is located to the South of the Campo dos Afonsos station and at 2 kilometers away from the shoreline, meteorological observations were realized only between 6 a.m. and 10 p.m. local time. In this station, it is possible to observe mainly the South direction, related to the sea breeze, and North direction, related to the land breeze (Figure 8). The occurrence of low-speed winds and the high percent of calm winds (10.15%) in the period of the study should be highlighted (Figure 8). Although it does not present the highest frequency specifically for the southern winds, it appears that the model represents the phenomenon of the sea breeze at a frequency like that observed, if assuming the southeast winds as one of the possible consequent directions of this phenomenon. It should also be noted that the northern winds associated with the land breeze are represented by the model at a frequency like the observation (Figure 8). Note that the WRF model simulates more intense winds than those observed, as well as verified for the SBGL station, and this average difference in intensity is about  $1.5 \text{ m.s}^{-1}$ . These are excellent results according to the criteria of Clifford (2011). However, it is noted that the model does not present good accuracy in representing calm winds for this site, *i.e.*, 3.9% modeled against 10.15% observed, the worst result among all sites.

The data observed at the Santa Cruz (SBSC) station, located on the West portion of the RJMR, near the Sepetiba bay, is presented in Figure 9. It can be noted that Southwest and Northeast winds are predominant due to the action of the land-sea and bay breeze circulations due to the presence of the Sepetiba bay and the Atlantic Ocean, besides the 8% of registered calm winds (Figure 9). Regarding the simulations, it is highlighted that the results demonstrate that the model could represent the phenomenon of the bay breeze associated with southwest winds. However, the present simulated results did not represent the wind direction associated with land breezes (northeastern winds) as good as the bay breeze (southwest winds) (Figure 9). The adequate simulation of the bay breeze represents a gain compared to the results from Paiva et al. (2014), who mentioned that the model fails to detect when the wind turns completely from the Southwest direction, even using numerical grids with higher horizontal resolution (300 m).

On the other hand, the high frequency of the north winds simulated by the WRF may be a model response to the present phenomenon since the meridional component of the wind has an important weight in the composition of the northeast winds. Other possibilities raised here are an excessive weight given by the model to the flow of synoptic-scale that produces winds from the north in this region, or even a flow-induced by mountain breezes to the north of this region (Aragão et al. 2017). Regarding the wind speed, both observed and modeled indicate that there are two most frequent classes, 2.1 to  $3.6 \text{ m.s}^{-1}$  and 3.6 to  $5.7 \text{ m.s}^{-1}$  (Figure 9). It is also verified that the model represents only about 50% of the cases of calms observed in the SBSC station.

In Table 3, the statistical indexes obtained for wind direction and speed are presented. As a most notable result, the bias index indicates a systematic trend of the model for all evaluated sites: a counterclockwise deviation of  $-4^\circ$  to  $-12^\circ$  about the wind direction observations. This trend of deviation in the wind direction agrees with the differences showed in the wind roses, where the model results always tend to deviate counterclockwise from observations, as demonstrated in the results for SBRJ, SBJR, and SBSC stations (Figures 7-9), that is, the three stations most influenced by the land-sea breeze. This may be evidence that the model has difficulties in representing mesoscale systems such as breezes, which in turn, maybe due to the excess weight given to the synoptic forces, or even the poor representation of the land-sea temperature gradient, which was remarked by Dragaud et al., (2019) for the coastal region of Rio de Janeiro state. Considering the bias and RMSE indexes the wind speed results are better in general than those demonstrated in previous literature by Hanna and Yang (2001), Zhang et al. (2011), Paiva et al. (2014), and Yver (2013), even considering the FDDA technique applied in

Hanna & Yang (2001) and the RJMR ultra-high-resolution surface databases used by Paiva et al. (2014). The values for bias evidence a slight overestimation of the simulated winds. According to Jiménez and Dudhia (2012b), this pattern of stronger simulated winds is frequently located over plains and valleys in complex terrain regions. Based on the criteria established by Clifford (2011) (Table 2), it can be verified in Table 3 that during the five months where the WRF model skill was evaluated its simulated results were considered excellent. The only exception was the RMSE index for SBSC (Table 3), considered a good result according to Clifford (2011). Since the results obtained through the WRF model demonstrate satisfactory performance and even superior to studies with ultra-high resolution and FDDA, it is assumed that the uncertainties from the atmospheric model are acceptable for air quality modeling.

Table 3  
Statistical indexes for surface winds simulated with the WRF.

Stations	Wind speed (m.s <sup>-1</sup> )			Wind direction (°)		
	bias	MAE	RMSE	bias	MAE	RMSE
SBGL	-1.00	1.46	1.85	-10.27	56.52	73.77
SBRJ	0.25	1.36	1.80	-4.32	52.01	71.65
SBAF	0.07	1.15	1.51	-7.42	67.40	85.08
SBJR	0.96	1.34	1.69	-12.57	53.74	73.93
SBSC	0.32	1.61	2.10	-12.47	60.79	80.09

## 4.2. Evaluation of the SO<sub>2</sub> hourly average concentrations results by using CONFIG1, CONFIG2, and CONFIG3

In Table 4, the statistical results for the simulated concentrations with CONFIG1, CONFIG2, and CONFIG3, at each AQ monitoring stations are shown. The analysis related to the NMSE index demonstrates that the CONFIG3 performs better in all AQ stations and the CONFIG1 presents the worst results except for the São Cristóvão station. It should also be noted that the NMSE values obtained for CONFIG3 are of the same order of magnitude or lower than those obtained by Cui et al. (2011), a study developed for the region of the Gan Jiang River, in China, whose values varied between 3 and 6. Systematically, all values for the bias index are positive, with CONFIG2 results being the worst of the three settings strategies. Although the bias indicates that the simulations overestimated the concentrations observed, the FOEX index demonstrates that the number of overestimated events (hours) is not always more frequent than the underestimated events. In this case, the results obtained for the Jardim Primavera station stand out, in which the underestimated events for CONFIG1 and CONFIG3 occur in 69% and 65% of the cases. In addition to this station, CONFIG1 also underestimated the concentrations observed at São Cristóvão station in 55% of cases. Still discussing FOEX, the results indicate that CONFIG3 presents the best balance between the number of underestimated and overestimated events.

Regarding the FA2 and FA5 indexes, in general, the results presented for CONFIG3 are also better, while the results for CONFIG2 are the worst. Despite important recent advances in atmospheric models, it is noted that the isolated use of simulated results in AQ models may not be the best strategy. The values of FA2 and FA5 attained through CONFIG3 suggest a better representation of the simulated pollutant dispersion than those obtained by Cui et al. (2011). Its maximum values were 27% and 61% for FA2 and FA5, respectively, which reinforces the

model's inclination to better results with this setting strategy. The standard deviation analysis indicates that, for all air quality monitoring stations, the magnitude of the simulated index is higher than that observed with the air quality monitoring data, with greater discrepancy on the Jardim Primavera and São Bento stations.

The results for the R index (Table 4) and the daily cycle of SO<sub>2</sub> (Fig. 10) demonstrate that the simulations are outdated in relation to that observed for all air quality monitoring stations, and there is a significant overestimation of the SO<sub>2</sub> concentration for the stations of São Cristóvão, São Bento and Jardim Primavera. It is not surprising the R index values close to 0, since the present evaluation is audacious in the sense of trying to model a highly urban environment with infinite casualties, unlike well-controlled experiments. However, the decision to present the correlation result is to encourage future studies and more investments in the data used in non-steady-state dispersion models. To be successful in modeling the variability of pollutant concentrations in the atmosphere, two main factors must be well represented: (1) emissions and, (2) advective and turbulent transport.

The first and perhaps the most important factor that impacts the correlation index is associated with the better representation of temporal variability of the emission sources. Although SO<sub>2</sub> vehicular emissions are small compared to fixed sources, and there is an hourly function for these emissions in the model, it is still an average representation, which does not include casual traffic jams, traffic diversions, and the difference between weekdays and weekends. Then, it's not surprising that there are lags between the maximum and minimum values and discrepancies in the intensity between the simulated and observed hourly concentration, as shown in Figure 10. As for industrial sources, probably they are not responsible for the poor correlation found, since the oil refineries are the main sources of SO<sub>2</sub> in RJMR and operate at constant load (INEA 2010), with exceptions for eventual maintenance.

The second factor is related to pollutant transport. Based on WRF results, the advective transport was satisfactorily represented in the present study. The turbulent transport and the atmospheric stability were not evaluated in this study, but as the representation of vehicle emissions, they can be sources of uncertainty. However, the investigation of these factors deserves further specific study using other data sources (*e.g.*, SODAR, micrometeorological stations, etc.). Improvements in the meteorological monitoring network could also bring gains in transport representation. The use of meteorological data with higher temporal resolution would allow the simulation of the transient effects of greater frequency (< 1 h), and more meteorological stations could accurately represent the spatial inhomogeneities of the area.

Table 4  
Statistical results for CALPUFF's SO<sub>2</sub> hourly concentrations.

AQ Stations	Std. dev. (µg.m <sup>-3</sup> )	Runs	Std. dev. (µg.m <sup>-3</sup> )	NMSE	Bias (µg.m <sup>-3</sup> )	FOEX (%)	FA2 (%)	FA5 (%)	R
Copacabana	2.52	CONFIG1	4.63	2.33	1.61	1.00	39.0	77.0	0.16
		CONFIG2	4.72	2.02	1.86	3.00	38.0	76.0	0.17
		CONFIG3	4.02	1.79	1.25	0.00	41.0	80.0	0.20
São Cristóvão	6.46	CONFIG1	8.68	3.19	1.31	-5.00	40.0	75.0	0.10
		CONFIG2	19.92	5.49	13.85	16.00	33.0	66.0	0.05
		CONFIG3	9.08	3.15	3.20	5.00	43.0	79.0	0.08
Tijuca	3.54	CONFIG1	5.07	2.35	0.68	-9.00	28.0	62.0	0.18
		CONFIG2	5.78	2.09	2.40	5.00	33.0	68.0	0.18
		CONFIG3	5.11	1.84	1.77	4.00	35.0	70.0	0.20
Jardim Primavera	3.01	CONFIG1	10.54	8.70	2.68	-19.00	33.0	69.0	0.05
		CONFIG2	16.69	8.18	10.31	6.00	32.0	68.0	0.00
		CONFIG3	9.38	5.44	2.21	-15.00	33.0	73.0	0.06
São Bento	5.35	CONFIG1	13.78	7.59	6.71	6.00	32.0	68.0	0.08
		CONFIG2	17.23	6.31	11.35	13.00	27.0	57.0	0.11
		CONFIG3	15.14	5.16	8.44	8.00	32.0	66.0	0.16

The bias of hourly wind speed and hourly SO<sub>2</sub> concentrations by observed wind speed categories (Figure 11) reveals important information that can contribute to a better understanding about the model errors and consequently indicate possible paths to be taken in future studies. According to Figure 11 left, it is observed that the smallest errors in wind intensity occur between 0.5 - 5.7 m·s<sup>-1</sup>, whereas high deviations occur for the calm winds and speeds above 5.7 m·s<sup>-1</sup>. It is noteworthy that no significant differences were found between the three configurations evaluated. Note that for the wind class with the smallest bias (2.1 - 3.6 m·s<sup>-1</sup>) (Figure 11, left), the smallest deviations for SO<sub>2</sub> concentration also occur, mainly for CONFIG1 and CONFIG3 (Figure 11, right). Despite the similar bias values regarding the wind speed among the three configurations (Figure 11, left), CONFIG2 presents the biggest discrepancies for SO<sub>2</sub> concentration (Figure 11, right). These analyzes highlight the importance of a meteorological monitoring network representative for wind and micrometeorological conditions.

### 4.3 Outlook for regulatory purposes

For regulatory purposes, the air quality standards in Brazil for the sulfur dioxide pollutant are established for 24-hour (125 µg.m<sup>-3</sup>) and annual sampling times (40 µg.m<sup>-3</sup>). Thus, in this section the results are analyzed considering the comparison between the simulated and observed average concentrations of 24 h, for the entire period of analysis, aiming to establish the performance of the CAQMS for practical applications.

In general, from the perspective of the evaluation of meteorological configurations among the simulations for regulatory purposes (Table 5 and Figure 12), a similar pattern of results was obtained for average hourly concentrations (Table 4). The best performances were obtained for configurations that used observed meteorological data (CONFIG1 and CONFIG3), with a slight superiority for CONFIG3. However, it is notable that the results for 24-hour averages (Table 5) are significantly better than those presented for hourly averages (Table 4). This corroborates with the previous argument that the difficulty of representing meteorological and emissions variations on minutes to hours scales impacts the results of the simulations.

As can be seen in Table 5 and Figure 12, the simulation results overestimate the average concentrations over the entire period at all air quality monitoring stations. It is evident in Figure 12 that the simulated concentrations rarely underestimate the observed concentrations. This result is reinforced by the overall positive bias index, whose all values are positive. Another information presented that is of paramount importance for regulatory studies is the model's ability to represent the maximum concentrations. As shown in Table 5, all maximum concentrations simulated overestimated those observed, reinforcing the tendency for overestimations. These errors follow the concentration levels of the stations, that is, the higher the concentration level at the station, the greater the associated error. Despite the models showing a positive bias, the simulated concentrations did not exceed the national air quality standard, in agreement with what was observed (Table 5).



Table 5

Statistical results for CALPUFF's daily averaged SO<sub>2</sub> concentrations ( $\mu\text{g}\cdot\text{m}^{-3}$ ).

AQ Stations	Mean/Max Obs. ( $\mu\text{g}\cdot\text{m}^{-3}$ )	Runs	Mean/Max Sim. ( $\mu\text{g}\cdot\text{m}^{-3}$ )	NMSE	bias ( $\mu\text{g}\cdot\text{m}^{-3}$ )	FOEX (%)	FA2 (%)	FA5 (%)	R
Copacabana	3.83 / 14.08	CONFIG1	5.41 / 17.28	0.76	1.54	14.0	58.0	95.0	0.09
		CONFIG2	5.69 / 16.73	0.59	1.83	18.0	61.0	96.0	0.31
		CONFIG3	5.06 / 16.89	0.52	1.21	11.0	69.0	97.0	0.30
São Cristóvão	8.36 / 25.16	CONFIG1	9.49 / 36.09	0.79	1.09	-2.0	56.0	90.0	0.03
		CONFIG2	21.64 / 61.71	1.44	13.24	44.0	40.0	79.0	0.16
		CONFIG3	11.27 / 37.53	0.72	2.67	9.0	64.0	93.0	0.03
Tijuca	4.45 / 14.55	CONFIG1	5.12 / 19.82	0.68	0.73	4.0	53.0	96.0	0.31
		CONFIG2	6.86 / 17.74	0.56	2.46	26.0	60.0	93.0	0.41
		CONFIG3	6.27 / 22.11	0.50	1.82	23.0	64.0	96.0	0.45
Jardim Primavera	6.47 / 21.39	CONFIG1	9.32 / 53.37	1.78	2.87	-5.0	47.0	88.0	0.14
		CONFIG2	16.85 / 63.42	2.41	10.49	30.0	39.0	80.0	-0.03
		CONFIG3	8.84 / 44.15	1.43	2.43	-3.0	47.0	88.0	0.06
São Bento	6.19 / 27.56	CONFIG1	12.84 / 55.08	1.78	6.67	25.0	47.0	80.0	0.13
		CONFIG2	17.72 / 50.10	1.96	11.45	36.0	32.0	71.0	0.23
		CONFIG3	14.74 / 45.12	1.45	8.45	33.0	42.0	81.0	0.36

Figure 13 reinforces what has already been shown in Figure 12. In the study region, SO<sub>2</sub> levels remain predominantly below 6  $\mu\text{g}\cdot\text{m}^{-3}$  in 24 hours (~ 65%), that is, in the lowest frequency classes of the graph (Figure 13). As for the bias of the simulations by frequency class, in general, the model errors more towards extreme concentrations, that is, tending to zero and >12  $\mu\text{g}\cdot\text{m}^{-3}$  (Figure 13). However, it should be noted that CONFIG3 has the smallest errors for the extremes, while CONFIG1 has the best performance for the intermediate classes. In all classes, CONFIG2 has the worst performance with errors twice as large as CONFIG1 and CONFIG3 in most concentration frequency classes.

## 5. Conclusions

The study demonstrates that the configuration of the WRF model for the RJMR was successful in the representation of the near-surface wind field. An evaluation was carried out for a robust period of 5 months in which a satisfactory agreement was demonstrated between the prevailing winds and the simulated winds by frequency distribution analysis. In a complementary way, it was found that the results from the statistical analysis, showed a model performance comparable to and even superior to other studies, including a study carried out by Paiva et al. (2014) for the same region using a higher resolution of terrain databases and horizontal grid resolution of the model with 300 m. It is worth remembering that RJMR is recognized for its high physiographic complexity, which makes the results found even more relevant. An important highlight that remains for future studies is the indication that the mesoscale forcing (land/sea breeze) is underestimated in relation to the synoptic forcing (SASA), or the latter is overestimated.

Regarding the best meteorological configuration for the CAQMS, there is a noticeable improvement of the obtained results with CONFIG3 when compared to the other configurations, indicating a positive influence considering both observational and simulated meteorological information that reinforces its better physical representation of the dispersion process of SO<sub>2</sub> on RJMR. On the other hand, it was found that the worst results were obtained with CONFIG2, which only includes the data from the WRF model. Although the WRF's performance was satisfactory, this result reinforces the importance of making investments in meteorological monitoring.

As for the skill of the CAQMS to simulate hourly SO<sub>2</sub> concentrations in RJMR, in general, the concentrations simulated overestimated the observed data. The results for the R index exposed the challenge in the temporal representation of the observed concentrations (on the hourly scale). The hypothesis is that the main source of uncertainties is the limited representativeness of the emissions regarding time variability. Besides, the unavailability of high-frequency meteorological data that records the transients in intra-hourly variability could also bring gains in transport representation. This theme merits a deep investigation, also expanding the analysis to other variables such as atmospheric stability. To encourage future studies, recently, two SODAR were installed in strategic sites in RJMR that could contribute significantly to the atmospheric conditions' assessment on pollutant concentration fields. However, the present results are very promising, since the region has rough terrain setting, non-homogenous soil use and occupation, presence of water bodies, time–space-varying emissions originated from several source types, besides the casualties about a highly urbanized region. The performance of the present study is comparable to Cui et al. (2011), who developed a study with controlled emissions, different from the current study that tried to represent the main anthropogenic emissions.

From a regulatory point of view, where the average concentrations are assessed in 24 hours for SO<sub>2</sub>, there was a significant improvement in the results towards those obtained for hourly averages. This result indicates a great potential of the WRF/CALMET/CALPUFF modeling system for regulatory purposes, where the concentrations are evaluated for averages greater than 1 hour for most pollutants. Since RJMR has a high degree of physiographic complexity and consequently a heterogeneous wind field, it is recommended that the competent environmental agencies review the current policies, who end up recommending the use of steady-state Gaussian models indiscriminately without specific legislation. The WRF/CALMET/CALPUFF air quality regulatory modeling system has proven to be an essential tool for environmental licensing studies and subsidized land use policies in Brazilian Metropolitan Regions aiming to achieve the UN 2030 Agenda goals.

# Declarations

**Availability of data and materials:** The datasets used and analyzed during the current study are available from the corresponding author on reasonable request.

## Author Contributions

Mauricio Soares da Silva: Conceptualization, Methodology, Software, Formal analysis, Investigation, Data Curation, Writing - Original Draft, Writing - Review & Editing and Visualization.

Luiz Claudio Gomes Pimentel: Conceptualization, Methodology, Validation, Formal analysis, Investigation, Resources, Writing - Original Draft, Writing - Review & Editing, Supervision, Project administration.

Fernando Pereira Duda: Conceptualization, Formal analysis and Writing - Review & Editing.

Leonardo Aragão: Methodology, Validation, Formal analysis, Investigation, Resources, Writing - Review & Editing.

Corbiniano Silva: Resources, Writing - Original Draft, Writing - Review & Editing, Visualization.

Ian Cunha D'Amato Viana DRAGAUD: Methodology, Investigation, Writing - Review & Editing.

Pedro Caffaro Vicentini: Data Curation, Methodology, Investigation, Writing - Review & Editing.

**Ethics approval and consent to participate:** Not applicable.

**Consent for publication:** Not applicable.

**Conflict of interest:** The authors declare no competing interests.

## ACKNOWLEDGMENTS

The INEA (State Environmental Institute) and SMAC (Municipal Secretary of the Environment of Rio de Janeiro) by the air quality monitoring data.

**Funding:** This work was conducted during a scholarship supported by the CAPES (Brazilian Federal Agency for Support and Evaluation of Graduate Education within the Ministry of Education of Brazil) and CNPQ (National Council for Scientific and Technological Development) at the Federal University of Rio de Janeiro.

# References

1. Abdul-Wahab AS, Ali S, Sardar S, Irfan N, Al-Damkhin A (2011a) Evaluating the performance of an integrated CALPUFF-MM5 modeling system for predicting SO<sub>2</sub> emission from a refinery. *Clean Technol Environ Policy* 13:841–854. <https://doi.org/10.1007/s10098-011-0360-6>
2. Abdul-Wahab S, Sappurd A, Al-Damkhi A (2011b) Application of California Puff (CALPUFF) model: a case study for Oman. *Clean Technol Environ Policy* 13:177–189. <https://doi.org/10.1007/s10098-010-0283-7>
3. Ajtai N, Stefanie H, Botezan C, Ozunu A, Radovici A, Dumitrache R, Iriza-Burcă A, Diamandi A, Hirtl M (2020) Support tools for land use policies based on high resolution regional air quality modelling. *Land Use Policy*

95:103909. <https://doi.org/10.1016/j.landusepol.2019.03.022>

4. Aragão LFS, Di Sabatino S, Pimentel LCG, Duda FP (2017) Analysis of the internal boundary layer formation on tropical coastal regions using SODAR data in Rio de Janeiro (Brazil). *Int J Environ Pollut* 62:136–154. <https://doi.org/10.1504/IJEP.2017.089403>
5. Byun D, Schere KL (2006) Review of the governing equations, computational algorithms, and other components of the Models-3 Community Multiscale Air Quality (CMAQ) modeling system. *Appl Mech Rev* 55:51–77. <https://doi.org/10.1115/1.2128636>
6. Chandrasekar A, Philbrickb CR, Clarkc R (2003) Evaluating the Performance of a Computationally Efficient MM5/CALMET System for Developing Wind Field Inputs to Air Quality Models. *Atmospheric Environment* 37:3267–3276. [https://doi.org/10.1016/S1352-2310\(03\)00325-X](https://doi.org/10.1016/S1352-2310(03)00325-X)
7. Chen L, Li L, Yang X, Zhang Y, Chen L, Ma X (2019) Assessing the impact of land-use planning on the atmospheric environment through predicting the spatial variability of airborne pollutants. *Int J Environ Res Public Health* 16:172. <https://doi.org/10.3390/ijerph16020172>
8. Chen M (2020) Application of WRF: How to get better performance. National Center for Atmospheric Research, Boulder, CO, USA. [https://www2.mmm.ucar.edu/wrf/users/tutorial/202001/chen\\_best\\_practices.pdf](https://www2.mmm.ucar.edu/wrf/users/tutorial/202001/chen_best_practices.pdf)
9. Chow FK, Weigel AP, Street RL, Rotach MW, Xue M (2006) High-resolution large-eddy simulations of flow in a steep Alpine valley. Part I: Methodology, verification, and sensitivity experiments. *Journal of Applied Meteorology and Climatology* 45:63–86. <https://doi.org/10.1175/JAM2322.1>
10. Clifford KT (2011) WRF-Model Performance for Wind Power Forecasting in the Coast Ranges of Central California. Master's Theses, Department of Meteorology and Climate Science, San José State University, United States, 61 pages.
11. Cui H, Yao R, Xu X, Xin C, Yang J (2011) A tracer experiment study to evaluate the CALPUFF real time in a near-field complex terrain setting. *Atmospheric Environment* 45:7525–7532. <https://doi.org/10.1016/j.atmosenv.2011.08.041>
12. Daly A, Zannetti P (2007) Air Pollution Modeling – An Overview. Chapter 2 of AMBIENT AIR POLLUTION. Published by The Arab School for Science and Technology (ASST) (<http://www.arabschool.org.sy>) and The EnviroComp Institute (<http://www.envirocomp.org/>). (<http://home.iitk.ac.in/~anubha/Modeling.pdf>)
13. De Visscher A (2013) Air Dispersion Modeling: Foundations and Applications. JohnWiley & Sons, Inc., Hoboken, New Jersey. <https://doi.org/10.1002/9781118723098.app1>
14. Defourny P, Vancutsem C, Bicheron P, Brockmann C, Nino F, Schouten L, Leroy M (2006) Globcover: a 300 m global land cover product for 2005 using ENVISAT MERIS time series. Proceedings of ISPRS Commission VII Mid-Term Symposium: Remote Sensing, May 8-11, 2006, Enschede (NL)
15. Dereczynski CP, Menezes WF (2015) Meteorology of the Campos Basin. In: FALCÃO, A. & FERNANDEZ, M. (eds) Regional environmental characterization of the Campos Basin. Elsevier. 2, 1-54. <https://doi.org/10.1016/B978-85-352-9016-5.50001-2>
16. DNIT – Departamento Nacional de Infraestrutura de Transportes (2006) Traffic Studies Manual, Rio de Janeiro, RJ, Brasil. (in Portuguese)
17. Dourado M, Oliveira AP (2001) Observational description of the atmospheric and oceanic boundary layers over the Atlantic Ocean. *Revista Brasileira de Oceanografia* 49:49–59. <https://doi.org/10.1590/S1413->

18. Dragaud ICDV, Soares da Silva M, de Freitas Assad LP, Cataldi M, Landau L, Elias RN, Pimentel LCG (2019) The impact of SST on the wind and air temperature simulations: a case study for the coastal region of the Rio de Janeiro state. *Meteorol Atmos Phys* 131(4):1083–1097. <https://doi.org/10.1007/s00703-018-0622-5>
19. EEA - European Environment Agency (2011) The application of models under the European Union's Air Quality Directive: A technical reference guide. EEA Technical report No 10/2011, Luxemburgo, 72 p., doi:10.2800/80600. 2011. ISSN 1725-2237
20. Farr TG, Rosen PA, Caro E, Crippen R, Duren R, Hensley S, Kobrick M, Paller M, Rodriguez E, Roth L, Seal D, Shaffer S, Shimada J, Umland J, Werner M, Oskin M, Burbank D, Alsdorf D (2007) The shuttle radar topography mission. *Rev Geophys* 45(2). doi:10.1029/2005RG000183
21. Geai P (1985) Methode d'Interpolation et de Reconstitution Tridimensionnelle d'un Champ de Vent: le Code d'Analyse Objective MINERVE. Technical Report DE R/ H E/3, pp. 4e8
22. Goger B, Rotach MW, Gohm A, Stiperski I, Fuhrer O (2016) Current challenges for numerical weather prediction in complex terrain: Topography representation and parameterizations. In 2016 International Conference on High Performance Computing & Simulation (HPCS) (pp. 890-894). IEEE
23. Grell GA, Dudhia J, Schmitz R, McKeen SA, Frost G, Skamarock WC, Eder B (2005) Fully-coupled "online" chemistry within the WRF model. *Atmos Environ* 39:6957–6976. <https://doi.org/10.1016/j.atmosenv.2005.04.027>
24. Haupt SE, Hanna S, Askelson M, Shepherd M, Fragomeni M, Debbage N, Johnson B (2019a) 100 years of progress in applied meteorology. Part II: Applications that address growing populations. *A Century of Progress in Atmospheric and Related Sciences: Celebrating the American Meteorological Society Centennial*, Meteor. Monogr., No. 59, American Meteorological Society, <https://doi.org/10.1175/AMSMONOGRAPHS-D-18-0007.1>
25. Haupt SE, Rauber RM, Carmichael B, Knievel JC, Cogan JL (2019b) 100 years of progress in applied meteorology. Part I: Basic applications. *A Century of Progress in Atmospheric and Related Sciences: Celebrating the American Meteorological Society Centennial*, Meteor. Monogr., No. 59, American Meteorological Society, <https://doi.org/10.1175/AMSMONOGRAPHS-D-18-0004.1>
26. Haupt SE, Kosovic B, McIntosh S, Chen F, Miller K, Shepherd M, Williams M, Drobot S (2019c) 100 years of progress in applied meteorology. Part III: Additional applications. *A Century of Progress in Atmospheric and Related Sciences: Celebrating the American Meteorological Society Centennial*, Meteor. Monogr., No. 59, American Meteorological Society, <https://doi.org/10.1175/AMSMONOGRAPHS-D-18-0012.1>
27. Higgins CD, Adams MD, Réquia WJ, Mohamed M (2019) Accessibility, air pollution, and congestion: Capturing spatial trade-offs from agglomeration in the property market. *Land Use Policy* 84:177–191
28. Holmes NS, Morawska L (2006) A review of dispersion modelling and its application to the dispersion of particles: an overview of different dispersion models available. *Atmos Environ* 40:5902–5928. <https://doi.org/10.1016/j.atmosenv.2006.06.003>
29. Hong S-Y, Noh N, Dudhia J (2006) A new vertical diffusion package with an explicit treatment of entrainment processes. *Mon Weather Rev* 134:2318–2341. <https://doi.org/10.1175/MWR3199.1>
30. Iacono MJ, Delamere JS, Mlawer EJ, Shephard MW, Clough SA, Collins WD (2008) Radiative forcing by long-lived greenhouse gases: Calculations with the AER radiative transfer models. *J Phys Res* 113:D13103. <https://doi.org/10.1029/2008JD009944>

31. IBGE – Instituto Brasileiro de Geografia e Estatística (2020) Territorial Units at the Metropolitan Region Level. IBGE Automatic Recovery System - SIDRA. Available in: <https://sidra.ibge.gov.br/territorio#/N7>. Accessed: 11-Jun-2020. (In Portuguese)
32. INEA – Instituto do Meio Ambiente do Estado do Rio de Janeiro (State Environmental Institute) (2010) Annual Air Quality Report for the State of Rio de Janeiro - 2009. Rio de Janeiro, RJ – Brazil, 108 pages. (In Portuguese)
33. INEA – Instituto do Meio Ambiente do Estado do Rio de Janeiro (State Environmental Institute) (2015) Atlas of conservation units. Available in: [http://www.inea.rj.gov.br/cs/idcplg?IdcService=GET\\_FILE&dID=133385&dDocName=INEA0123044](http://www.inea.rj.gov.br/cs/idcplg?IdcService=GET_FILE&dID=133385&dDocName=INEA0123044). (In Portuguese)
34. Jackson B, Chau D, Gurer K, Kaduwela A (2006) Comparison of ozone simulations using MM5 and CALMET/ MM5 hybrid meteorological fields for the July/August 2000 CCOS episode. *Atmos Environ* 40:2812–2822. <https://doi.org/10.1016/j.atmosenv.2006.01.020>
35. Jiménez PA, Dudhia J, Gonzalez–Rouco JF, Navarro J, Montavez JP, Garcia–Bustamante E (2012a) A revised scheme for the WRF surface layer formulation. *Mon Weather Rev* 140:898–918. doi:10.1175/MWR-D-11-00056.1
36. Jiménez PA, Dudhia J (2012b) Improving the Representation of Resolved and Unresolved Topographic Effects on Surface Wind in the WRF Model. *Journal Applied Meteorology and Climatology* 51:300–316. <https://doi.org/10.1175/JAMC-D-11-084.1>
37. Klausmann AM, Groot W, Phadnis M, Scire JS (2003) A Real-Time Meteorological Analysis and Dispersion Prediction System for Emergency Preparedness. Nuclear Utility Meteorological Data User’s Group. 19 pages.
38. Lafortune G, Fuller G, Moreno J, Schmidt-Traub G, Kroll C (2018) SDG Index and Dashboards: detailed methodological paper. Bertelsmann Stiftung and Sustainable Development Solutions Network, Paris
39. Lalas DP, Ratto CF (1996) *Modelling of Atmospheric Flow Fields*, World Scientific. 753 pages
40. Lee H-D, Yoo J-W, Kang M-K, Kang J-S, Jung J-H, Oh K-J (2014) Evaluation of concentrations and source contribution of PM10 and SO2 emitted from industrial complexes in Ulsan, Korea: interfacing of the WRF-CALPUFF modeling tools. *Atmospheric Pollution Research* 5:664–676. <https://doi.org/10.5094/APR.2014.076>
41. Leelőssy Á, Molnár F, Izsák F, Havasi Á, Lagzi I, Mészáros R (2014) Dispersion modeling of air pollutants in the atmosphere: a review. *Open Geosciences* 6:257–278. <https://doi.org/10.2478/s13533-012-0188-6>
42. Mosca S, Graziani G, Klug W, Bellasio R, Bianconi R (1998) A statistical Methodology for the evaluation of long-range Dispersion models: an application to the ETEX Exercise. *Atmos Environ* 32:4307–4324. [https://doi.org/10.1016/S1352-2310\(98\)00179-4](https://doi.org/10.1016/S1352-2310(98)00179-4)
43. Niu G–Y, Yang Z–L, Mitchell KE, Chen F, Ek MB, Barlage M, Kumar A, Manning K, Niyogi D, Rosero E, Tewari M, Xia Y (2011) The community Noah land surface model with multiparameterization options (Noah–MP): 1. Model description and evaluation with local–scale measurements. *J Geophys Res* 116:D12109. <https://doi.org/10.1029/2010JD015139>
44. Oettl D (2013) Documentation of the Lagrangian Particle Model GRAL (Graz Lagrangian Model Vs. 13.3.Amt d. Stmk. Landesregierung, ABT15, Referat Luftreinhaltung, Bericht: Lu-03-12, 116 pp. [http://app.luis.steiermark.at/berichte/Download/Fachberichte/Lu\\_03\\_13\\_GRAL\\_Documentation.pdf](http://app.luis.steiermark.at/berichte/Download/Fachberichte/Lu_03_13_GRAL_Documentation.pdf)

45. Oliveri Conti G, Heibati B, Kloog I, Fiore M, Ferrante M (2017) A review of AirQ Models and their applications for forecasting the air pollution health outcomes. *Environ Sci Pollut Res* 24:6426–6445. <https://doi.org/10.1007/s11356-016-8180-1>
46. Paiva LM, Bodstein GCR, Pimentel LCG (2014) Influence of high-resolution surface databases on the modeling of local atmospheric circulation systems. *Geosci Model Dev* 7:1641–1659. <https://doi.org/10.5194/gmd-7-1641-2014>
47. Pardyjak ER, Brown M (2003) QUIC-URB v. 1.1: Theory and User's Guide. Los Alamos National Laboratory, Los Alamos, New Mexico, USA
48. Pfender W, Graw R, Bradley W, Carney M, Maxwell L (2006) Use of a complex air pollution model to estimate dispersal and deposition of grass stem rust urediniospores at landscape scale. *Agricultural and Forest Meteorology* 139:138–153. <https://doi.org/10.1016/j.agrformet.2006.06.007>
49. Pielke RA (2002) *Mesoscale Meteorological Modeling, Second Edition*, Academic Press. 676 pages
50. Pimentel LCG, Marton E, Soares da Silva M, Jourdan P (2014a) Characterization of surface wind regime in the Metropolitan Area of Rio de Janeiro. *Engenharia Sanitária e Ambiental* 19(2):121–132. <https://doi.org/10.1590/S1413-41522014000200003>(In Portuguese)
51. Pimentel LCG, Correa EB, Marton E, Cataldi M, Nogueira E (2014b) Influence of the configuration parameters of the CALMET model on the simulation of the atmospheric circulation in the metropolitan region of Rio de Janeiro. *Revista Brasileira de Meteorologia* [online]. 2014, vol.29, n.4, pp.579-596. ISSN 0102-7786. <http://dx.doi.org/10.1590/0102-778620130099>. (In Portuguese)
52. Pires DJ (2005) Stationary source atmospheric emission inventory and its contribution for the air pollution in the Rio de Janeiro Metropolitan region. Master's Theses, Department of Energy Planning. Federal University of Rio de Janeiro, Rio de Janeiro, RJ. Brazil, 188 pages. (In Portuguese)
53. Rafaj P, Kieseewetter G, Gül T, Schöpp W, Cofala J, Klimont Z, Purohit P, Heyes C, Amann M, Borken-Kleefeld J, Cozzi L (2018) Outlook for clean air in the context of sustainable development goals. *Glob Environ Change* 53:1–11. <https://doi.org/10.1016/j.gloenvcha.2018.08.008>
54. Requia WJ, Roig HL, Koutrakis P, Rossi MS (2016) Mapping alternatives for public policy decision making related to human exposures from air pollution sources in the Federal District, Brazil. *Land Use Policy* 59:375–385. <http://dx.doi.org/10.1016/j.landusepol.2016.09.017>
55. Rzeszutek M (2019) Parameterization and evaluation of the CALMET/CALPUFF model system in near-field and complex terrain - Terrain data, grid resolution and terrain adjustment method. *Science of the Total Environment* 689:31–46. <https://doi.org/10.1016/j.scitotenv.2019.06.379>
56. Scire JS, Robe FR, Fernau ME, Yamartino RJ (2000a) A User's Guide for the CALMET Meteorological Model (Version 5). Earth Tech Inc., Concord, MA, p 316
57. Scire JS, Strimaitis DG, Yamartino RJ (2000b) A User's Guide for the CALPUFF Dispersion Model (Version 5.0). Earth Tech, Inc., Concord, MA, p 468
58. Silveira VS, De Oliveira JF, Soares da Silva M, Silva C, Alves AR, Souza Pontes A, Pimentel LCG, Rotunno Filho OC (2021) Analysis of urban - industrial expansion and increasing level of ozone concentration as subsiding an environmental management plan for the east of Rio de Janeiro metropolitan area – Brazil, *Land Use Policy*. 101, 2021, 105 – 148. <https://doi.org/10.1016/j.landusepol.2020.105148>

59. Soares da Silva MS, Pimentel LCG (2017) Challenges and air quality control strategies in metropolitan regions. *Diversidade e Gestão*,1, 107-126. Volume Especial. *Perspectivas, Conceitos e Casos, Gestão Ambiental*. (in Portuguese)
60. Skamarock WC, Klemp JB, Dudhia J, Gill DO, Liu Z, Berner J, Wang W, Powers JG, Duda MG, Barker DM, Huang X-Y (2019) A Description of the Advanced Research WRF Version 4. *NCAR Tech. Note NCAR/TN-556+STR*, 145 pp. doi:10.5065/1dfh-6p97
61. Stech JL, Lorenzetti JA (1992) The response of the South Brazil Bight to the passage of wintertime cold fronts. *J Geophys Res* 97:9507–9520. <https://doi.org/10.1029/92JC00486>
62. Sykes R, Lewellen W, Parker S (1984) A turbulent-transport model for concentration fluctuations and fluxes. *J Fluid Mech* 139:193–218. doi:10.1017/S002211208400032X
63. Sykes RI, Parker SF, Henn DS, Gabruk RS (1996) SCIPUFF – A Generalized Dispersion Model.. In: Gryning SE, Schiermeier FA (eds) *Air Pollution Modeling and Its Application XI. NATO Challenges of Modern Society*, vol 21. Springer, Boston, MA. [https://doi.org/10.1007/978-1-4615-5841-5\\_45](https://doi.org/10.1007/978-1-4615-5841-5_45)
64. UN – United Nations (2015) Resolution Adopted by the General Assembly on 25 September 2015. *Transforming Our World: The 2030 Agenda for Sustainable Development*
65. UN – United Nations (2018) Department of economic and social affairs, population division. *The World's Cities in 2018 – Data Booklet (ST/ESA/ SER.A/417)*. Available: [https://www.un.org/en/events/citiesday/assets/pdf/the\\_worlds\\_cities\\_in\\_2018\\_data\\_booklet.pdf](https://www.un.org/en/events/citiesday/assets/pdf/the_worlds_cities_in_2018_data_booklet.pdf) Accessed: 21-Apr-2021
66. USEPA – United States Environmental Protection Agency (1995) *User's Guide for the Industrial Source Complex (ISC3) Dispersion Models (revised) Volume II – Description of Model Algorithms*, In: EPA-454/b-95-003b, North Carolina, U.S.A
67. USEPA – United States Environmental Protection Agency (2004) *AERMOD: Description of Model Formulation*. EPA-454/R-03-004. North Carolina, U.S. Environmental Protection Agency
68. Vicentini PC, Thesis (2011) Department of Mechanical Engineering, Federal University of Rio de Janeiro, Rio de Janeiro, Brazil, 224 pages
69. Vicentini PC, Pimentel LCG, Soares da Silva M, Souza Pontes A (2011) Effects of PROCONVE in the Metropolitan Region of Rio de Janeiro between 2008 and 2020 - Evaluation using an Emissions Inventory and an Air Quality Model. In: *XIX Simpósio Internacional de Engenharia Automotiva - SIMEA, 2011, 2011, São Paulo, SP. XIX Simpósio Internacional de Engenharia Automotiva - SIMEA, 2011. São Paulo, SP: SIMEA, 2011, 2011. v. I (in Portuguese)*
70. Yang D, Wang A, Zhang R (2008) Estimating Air Quality Impacts of Elevated Point Source Emissions in Chongqing, China. *Aerosol Air Qual Res* 8:279–294. <https://doi.org/10.4209/aaqr.2008.02.0005>
71. Yano JI, Ziemiański MZ, Cullen M, Termonia P, Onvlee J, Bengtsson L, Carrassi A, Davy R, Deluca A, Gray SL, Homar V, Köhler M, Krichak S, Michaelides S, Phillips VTJ, Soares PMM, Wyszogrodzki AA (2018) Scientific challenges of convective-scale numerical weather prediction. *Bull Am Meteorol Soc* 99(4):699–710. <https://doi.org/10.1175/BAMS-D-17-0125.1>
72. Yim SHL, Fung JCH, Lau AKH (2010) Use of high-resolution MM5/CALMET/CALPUFF system: SO<sub>2</sub> apportionment to air quality in Hong Kong. *Atmos Environ* 44:4850–5858. <https://doi.org/10.1016/j.atmosenv.2010.08.037>



73. Yver CE, Graven HD, Lucas DD, Cameron-Smith PJ, Keeling RF, Weiss RF (2013) Evaluating transport in the WRF model along the California coast. *Atmos Chem Phys* 13:1837–1852. <https://doi.org/10.5194/acp-13-1837-2013>
74. Wang S, Hao J (2012) Air quality management in China: Issues, challenges, and options. *Journal of Environmental Sciences*, v. 24(1), p. 2–13, 2012. [https://doi.org/10.1016/S1001-0742\(11\)60724-9](https://doi.org/10.1016/S1001-0742(11)60724-9)
75. WHO - World Health Organization (2016) Ambient air pollution: A global assessment of exposure and burden of disease. <https://apps.who.int/iris/handle/10665/250141>
76. WMO - World Meteorological Organization (2016) Guide to Meteorological Instruments and Methods of Observation, Volume I – Measurement of Meteorological Variables WMO-No. 8, 2018 edition, 548 pages
77. WMO - World Meteorological Organization (2018) Guide to Meteorological Instruments and Methods of Observation, Volume I – Measurement of Meteorological Variables WMO-No. 8, 2018 edition, 548 pages
78. Wu H, Zhang Y, Yu Q, MaW (2018) Application of an integrated WRF/CALPUFF modeling tool for source apportionment of atmospheric pollutants for air quality management: a case study in the urban area of Benxi, China. *J Air Waste Manag Assoc* 2247. <https://doi.org/10.1080/10962247.2017.1391009>
79. Zhang Y, Cheng S-H, Chen Y-S, Wang W-X (2011) Application of MM5 in China: Model evaluation, seasonal variations and sensitivity to horizontal grid resolutions. *Atmos Environ* 45:3454–3465. <https://doi.org/10.1016/j.atmosenv.2011.03.019>
80. WMO - World Meteorological Organization (2016) Guide to Meteorological Instruments and Methods of Observation, Volume I – Measurement of Meteorological Variables WMO-No. 8, 2018 edition, 548 pages.
81. WMO - World Meteorological Organization (2018) Guide to Meteorological Instruments and Methods of Observation, Volume I – Measurement of Meteorological Variables WMO-No. 8, 2018 edition, 548 pages.
82. Wu H, Zhang Y, Yu Q, MaW (2018) Application of an integrated WRF/CALPUFF modeling tool for source apportionment of atmospheric pollutants for air quality management: a case study in the urban area of Benxi, China. *Journal of the Air & Waste Management Association*, 2247. <https://doi.org/10.1080/10962247.2017.1391009>
83. Zhang, Y, Cheng S-H, Chen Y-S, Wang, W-X (2011) Application of MM5 in China: Model evaluation, seasonal variations and sensitivity to horizontal grid resolutions. *Atmospheric Environment*, 45, 3454-3465. <https://doi.org/10.1016/j.atmosenv.2011.03.019>

## Figures

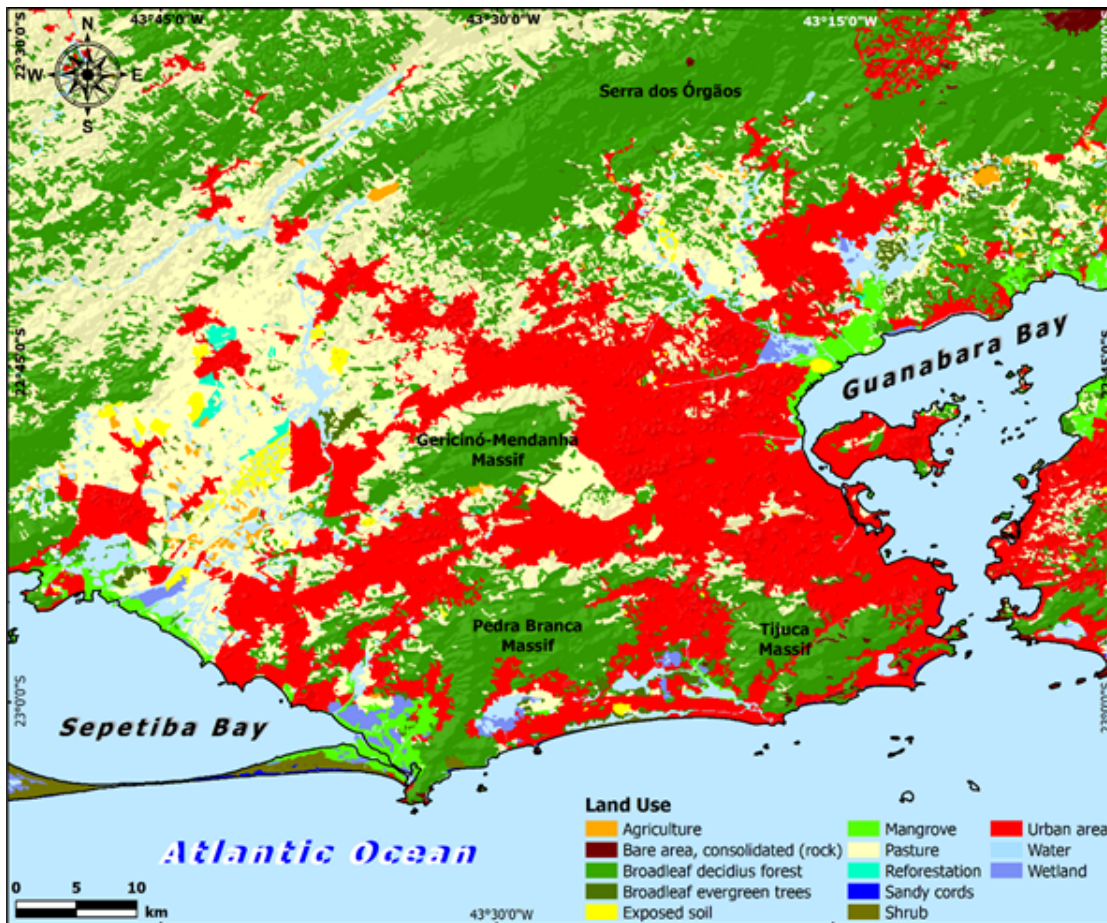


Figure 1

Study area, with emphasis on: Serra dos Órgãos mountain range to the north; Atlantic Ocean to the south; Gericinó-Mendanha, Pedra Branca and Tijuca massifs, and Guanabara and Sepetiba bays.



**Figure 2**

Topography and its main features, Meteorological, AQ monitoring, pluviometric stations, and SDGs.

**Figure 3**

Domain settings in the WRF model.

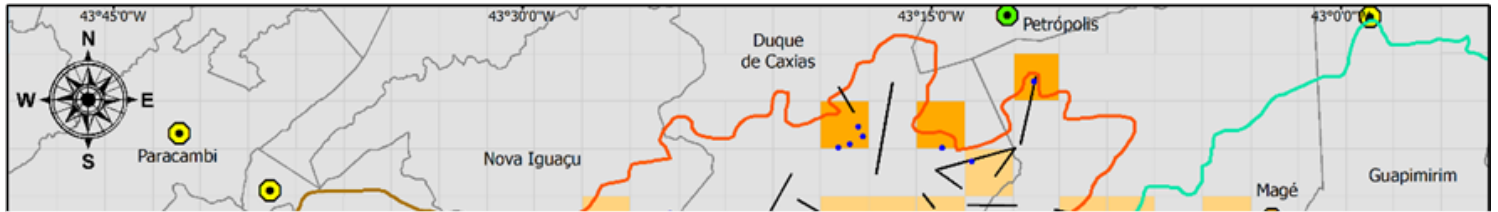


**Figure 4**

Spatial distribution of SO<sub>2</sub> total emissions by 5x5 km area for the RJMR (fixed/industrial and mobile/vehicular emissions).

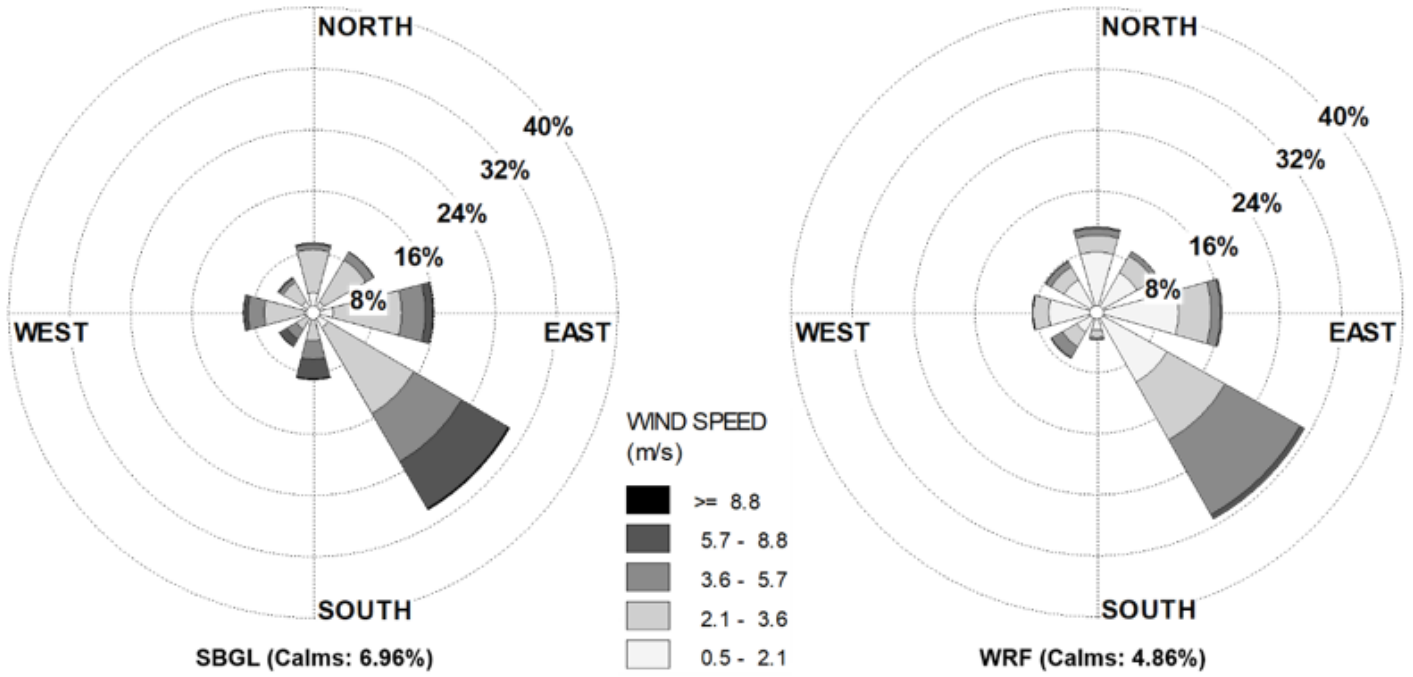


Figure 5

Frequency distribution diagrams evaluated for the Galeão station (SBGL). Observed (left) and modeled (right).

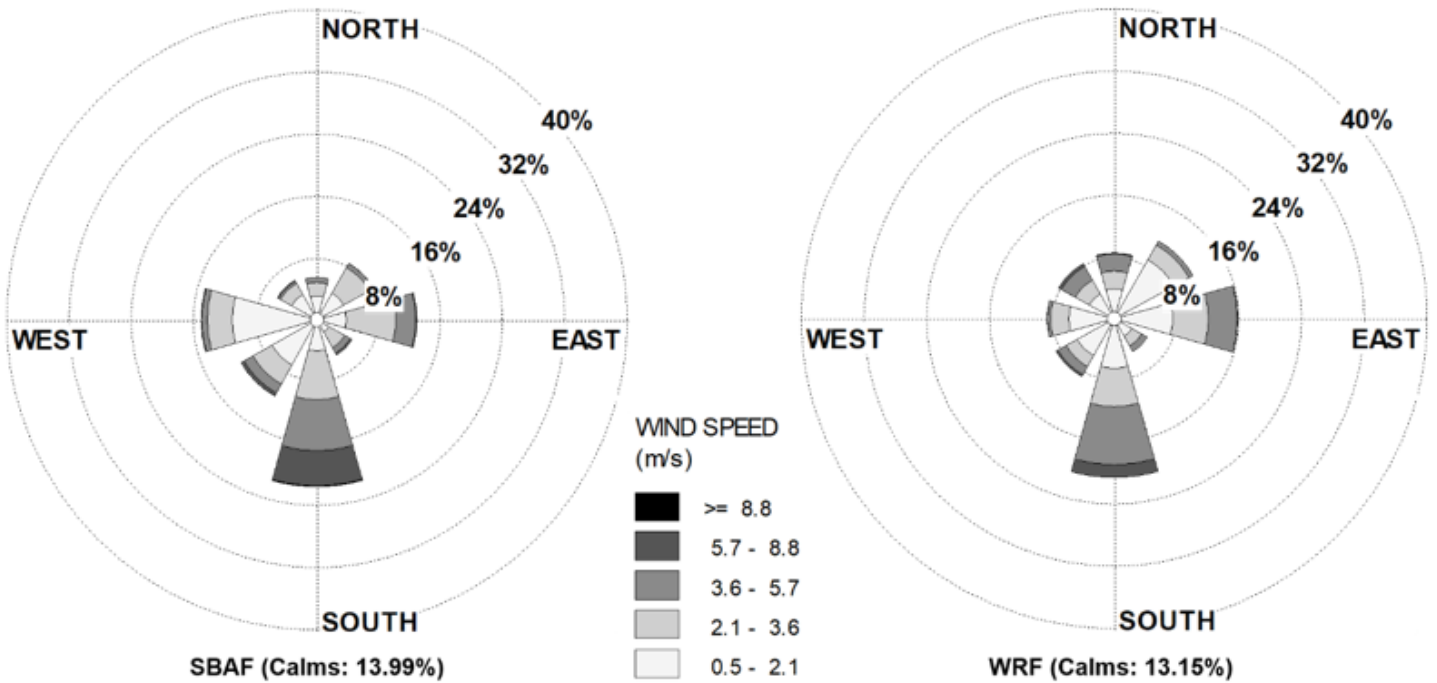


Figure 6

Frequency distribution diagrams evaluated for the Campo dos Afonsos station (SBAF). Observed (left) and modeled (right).

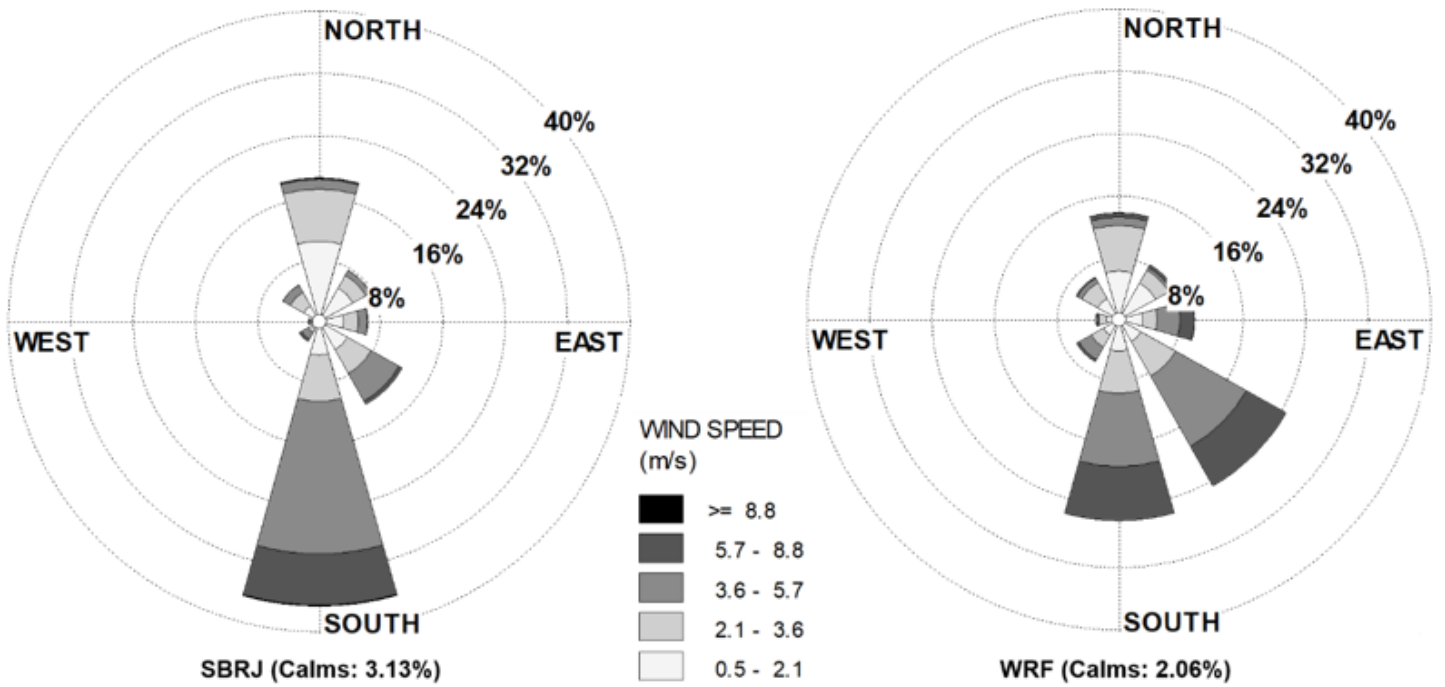


Figure 7

Frequency distribution diagrams evaluated for the Santos Dumont station (SBRJ). Observed (left) and modeled (right).

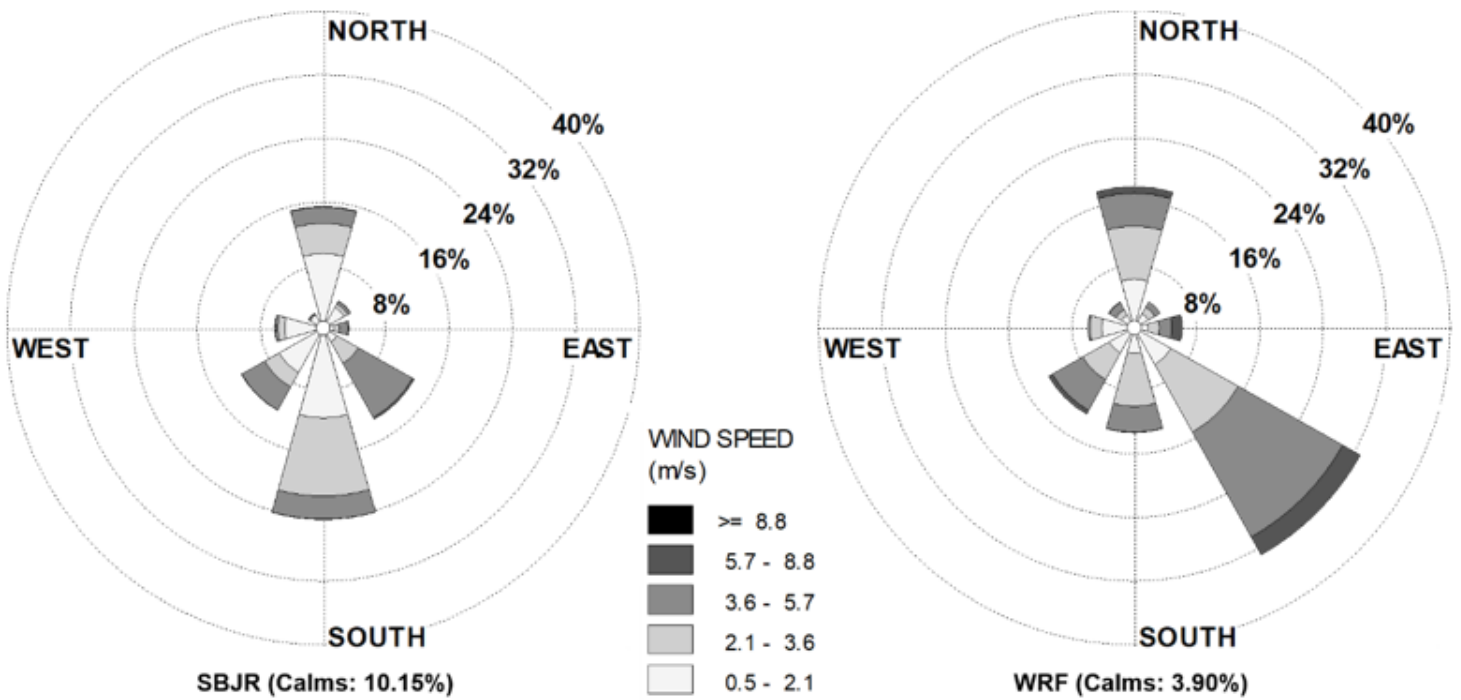


Figure 8

Frequency distribution diagrams evaluated for the Jacarepaguá station (SBJR). Observed (left) and modeled (right).

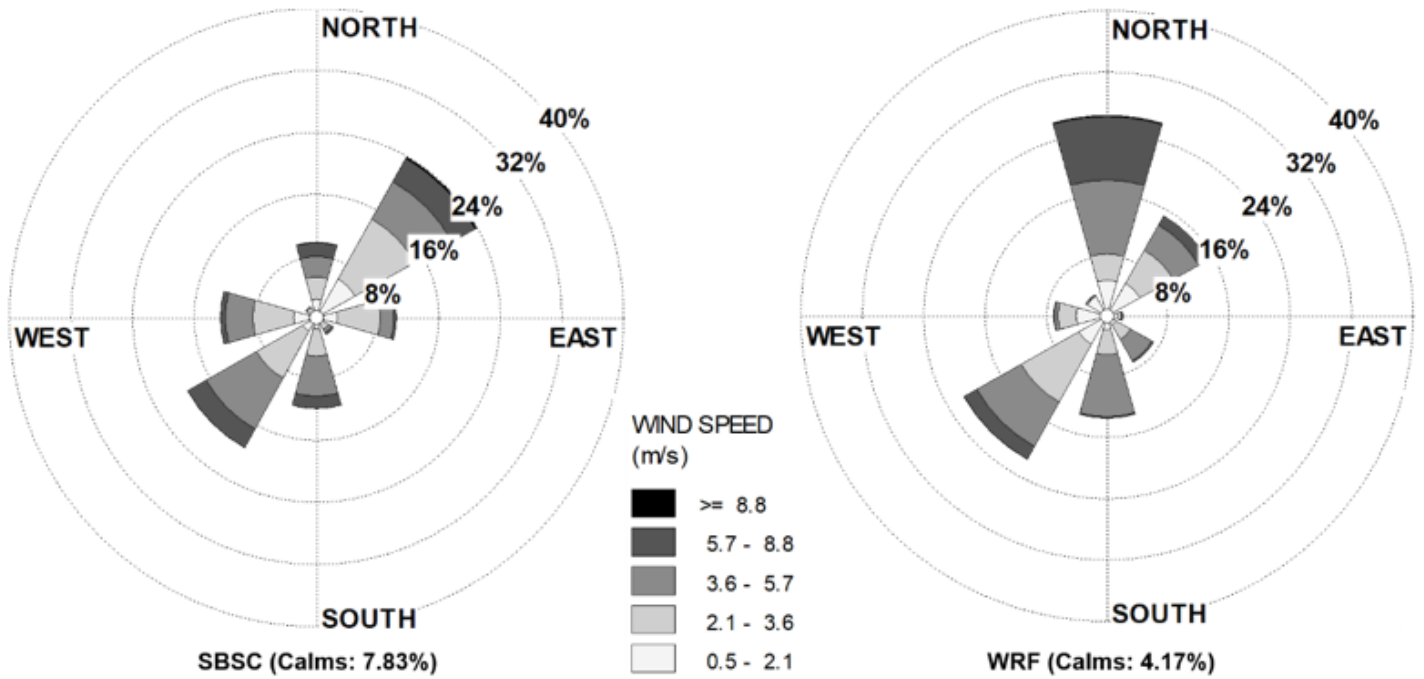
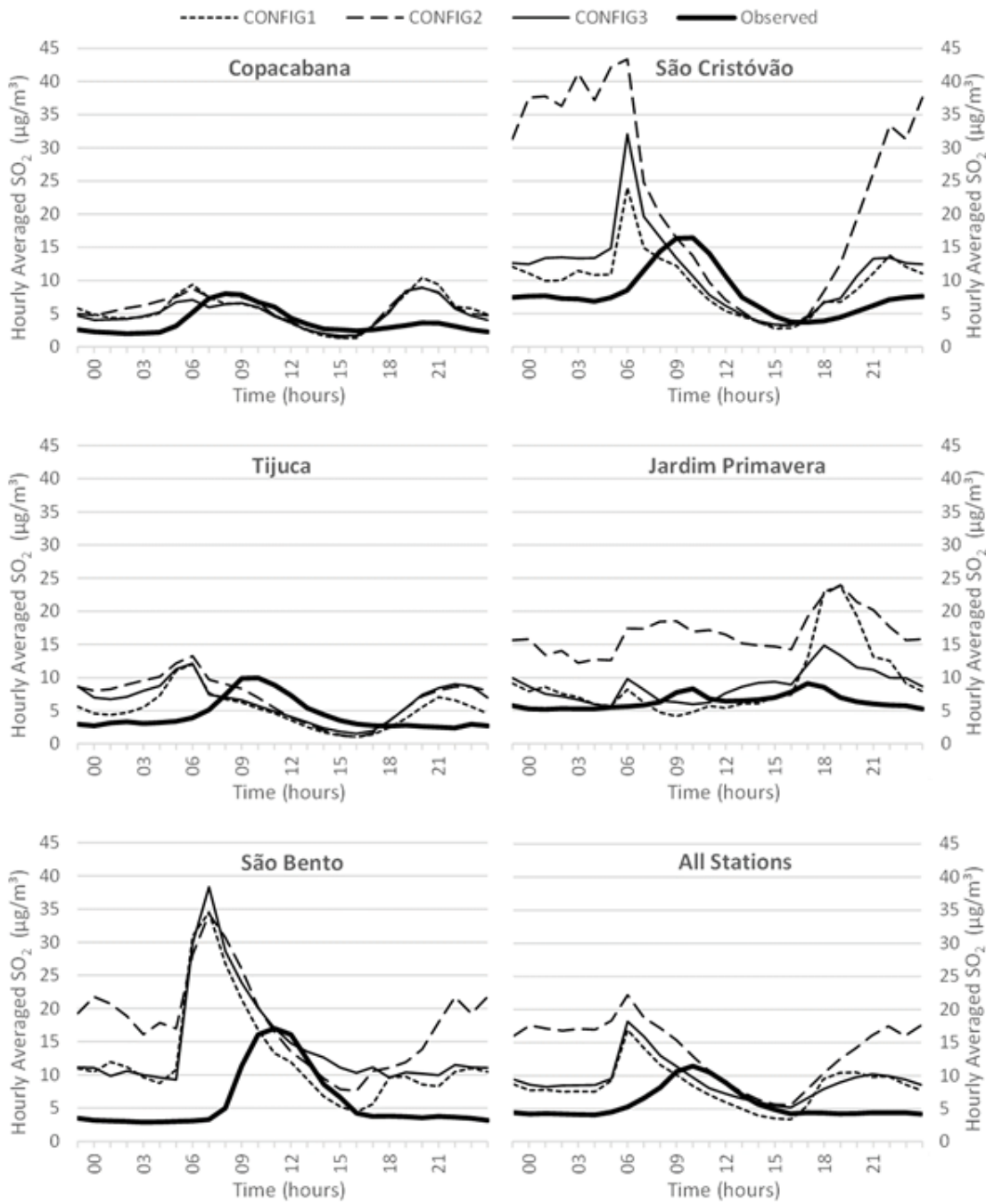


Figure 9

Frequency distribution diagrams evaluated for the Santa Cruz station (SBSC). Observed (left) and modeled (right).





**Figure 10**

The daily cycle of hourly averaged SO<sub>2</sub> concentrations (μg.m<sup>-3</sup>) observed in AQ stations and estimated by each CALPUFF configuration.



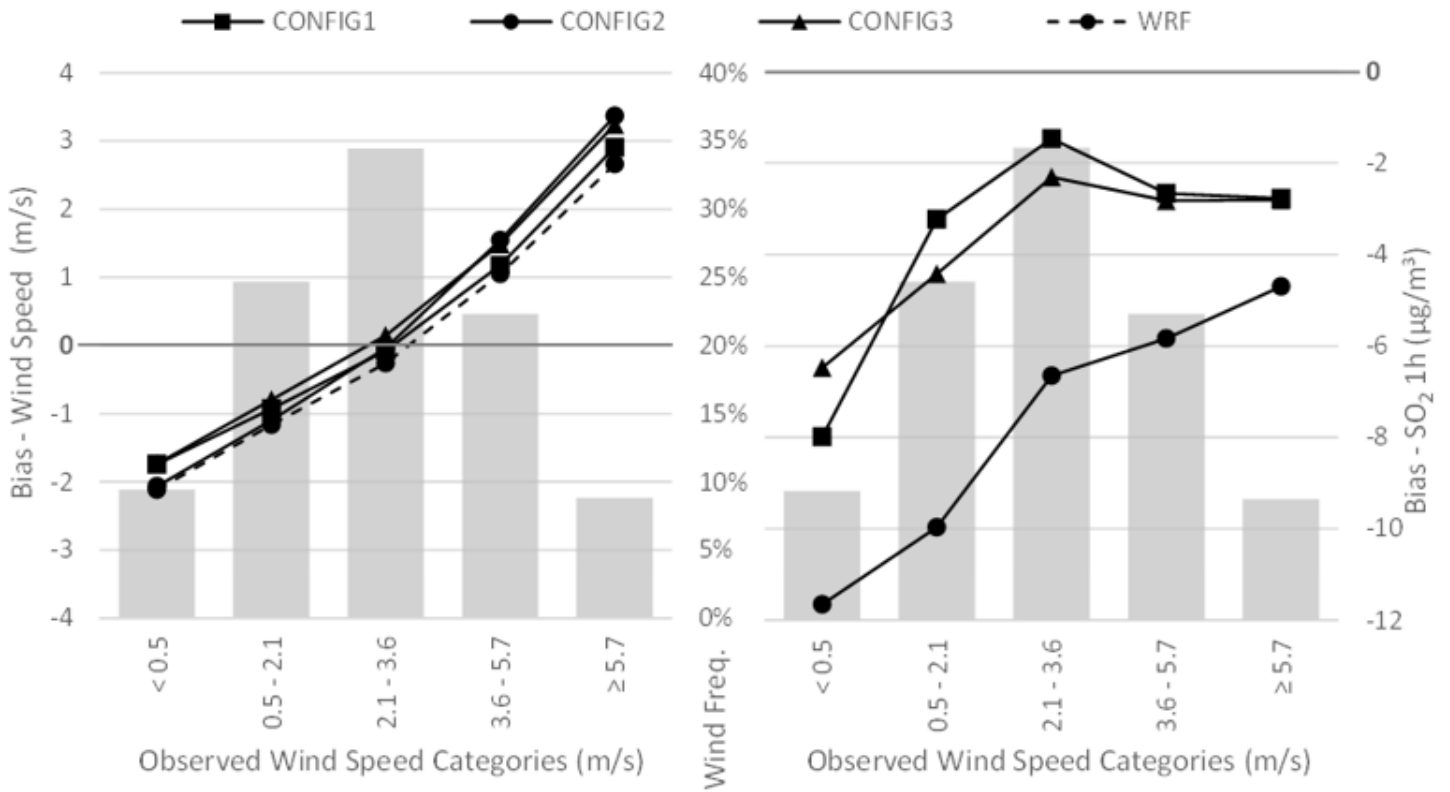


Figure 11

Frequency distribution of observed hourly wind speed (grey bars) by wind category, including bias of hourly wind speed estimated by each CALMET configuration and by WRF (left), and bias of SO<sub>2</sub> concentrations 1h (right) estimated by each CALPUFF configuration.

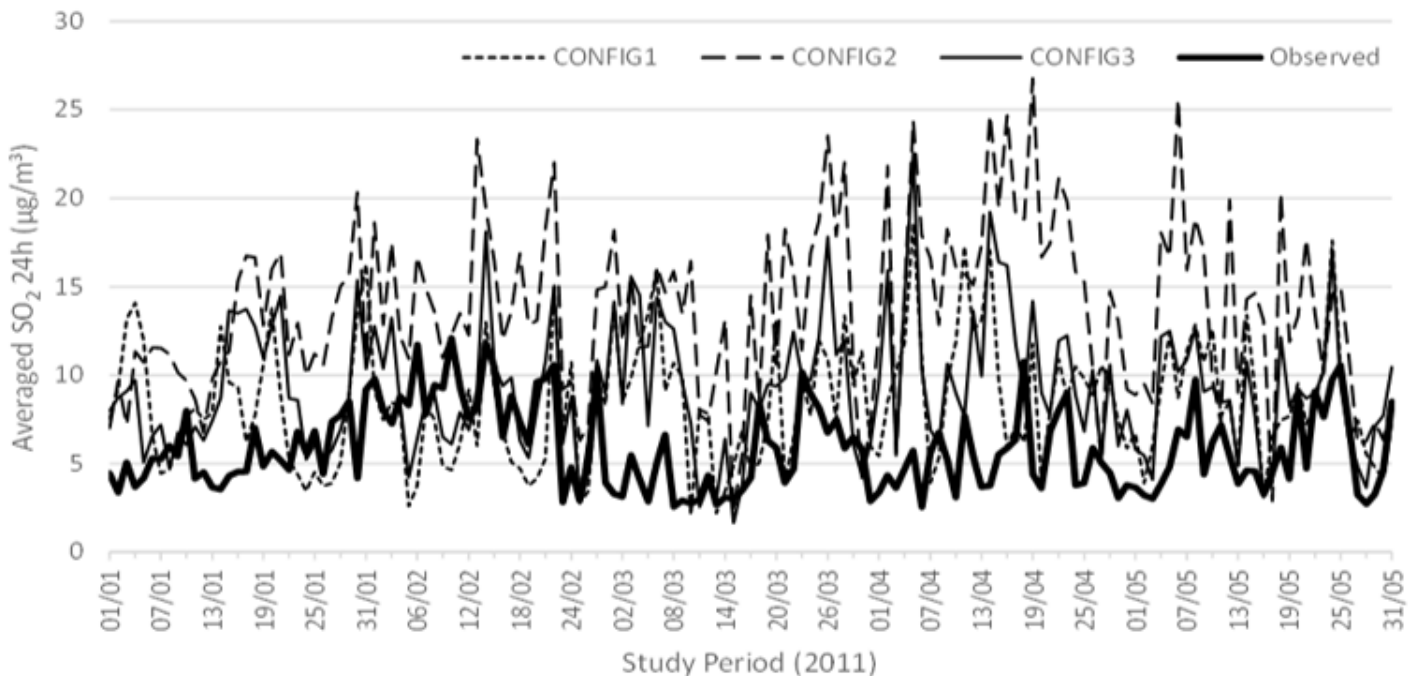
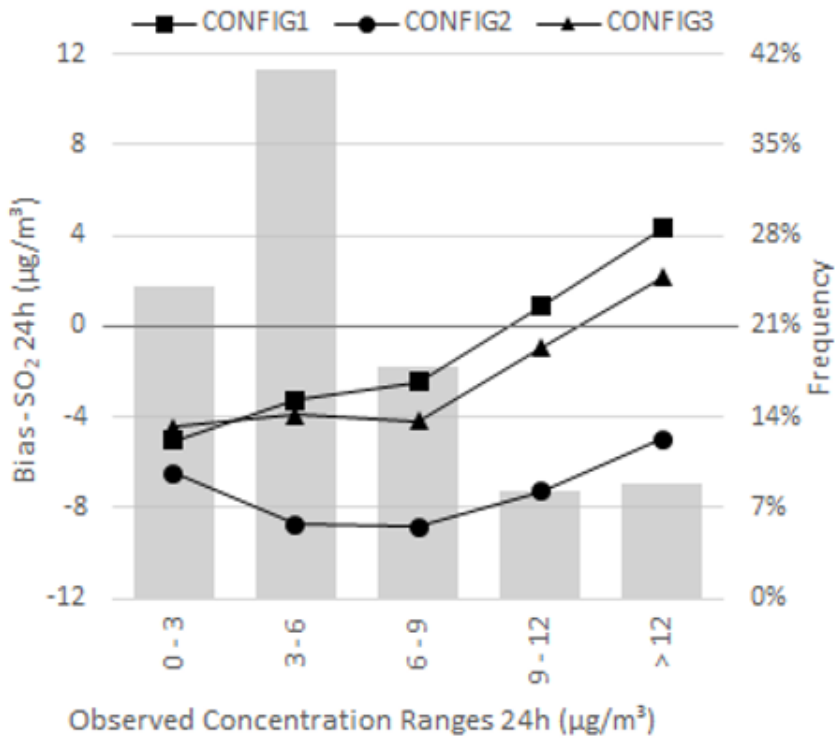


Figure 12

Timeseries of daily averaged SO<sub>2</sub> concentrations (µg.m<sup>-3</sup>) between all simulated (dashed lines) and observed (shaded lines) sites.



**Figure 13**

Frequency distribution of observed SO<sub>2</sub> concentrations (grey bars) in 24h, including bias of SO<sub>2</sub> concentrations estimated by each CALPUFF configuration.